ADDIS ABABA UNIVERSITY

SCHOOL OF GRADATE STUDIES

DEPARTMENT OF EARTH SCIENCES

GEOPHYSICAL INVESTIGATIONS TO STUDY THE GROUNDWATER CONTROLLING FACTOR

IN DEKA BORA-TULU REI SECTOR,

MOJO,

MAIN ETHIOPIAN RIFT

A Thesis Submitted to the School of Graduate Studies

Addis Ababa University

In Partial Fulfillment of the Requirements for the Degree of

Master of Science in Geophysics

By

MINILIK WUBE DESSALEGN

June 2005

ADDIS ABABA UNIVERSITY
SCHOOL OF GRADATE STUDIES
DEPARTMENT OF EARTH SCIENCES

GEOPHYSICAL INVESTIGATIONS TO STUDY THE GROUNDWATER CONTROLLING FACTOR

IN DEKA BORA-TULU REI SECTOR,

MOJO,

MAIN ETHIOPIAN RIFT

By

MINILIK WUBE DESSALEGN

Approval by board of examiners:

Dr. Dereje ayalew .....
Chairman
Dr. Tigistu Haile .....
Advisor
Dr. Shimels Fisseha .....
Internal Examiner
Dr. Getnet Mewa .....
External Examine

Acknowledgement

Many thanks Dr.Tigistu Haile, to my advisor and initiator of this work. His pleasant working atmosphere and way of guiding creates me a hardworking environment, which I am glad I was able to use. Further more I would like to thank him for sharing his knowledge; giving me reference materials and arranging my field trip, I appreciated that a lot.

I would like to express my sincere gratitude to Benishangul Gumuz Regional State Water Mines and Energy Development Bureau for the voluble sponsorship granted for my study. The Department of Earth Science of Addis Ababa University also share my great thanks for providing financial assistance and allowing me to undertake this research

I would also like to acknowledge the Department of Earth Science and the staffs; particularly, Dr. Tamara Alemayehu, Dr. Telahun Mammo, Dr. Shimeles and non staffs geophysics professionals; Ato Tibebe, Ato Ali and Ato Moges Tigabe for their dedication in delivery of the subject matter and unreserved sharing in their field of experience.My deepest heart felt thank goes to may family for their priceless effort in educating me since my childhood.

Finally my deep appreciation goes to my family for their priceless effort in educating in educating me since my childhood.

Table of Contents

LIST OF TABLES AND FIGURES

ABSTRACT

This work presents the results of combined electrical resistivity and gravity surveys carried out over two rural communities of Deka Bora and Tulu Rie, two largely populated rural communities on the Mojo-shenkora road, with the objective of locating preferred borehole sites for the extraction of groundwater for livestock and domestic use.

The areas found in the western margin of Main Ethiopian Rift are rich in agricultural products but are in severe shortage of drinking water for most part of the year. Several attempts by various governmental and non governmental agencies to extract water from the subsurface have failed. Within these locations and in areas close by even and deep wells have failed to tap groundwater and the search for groundwater has almost been abandoned in resent times. It was the first objective of the work to minimize the risk of sinking dry wells by assessing groundwater.

It was found from the work that the major groundwater controlling factors are structural and a detailed study of these structures and accurate location of the preferred borehole site are essential for groundwater search and drilling work to succeed. The work has also located some important potential areas for drilling and extraction of groundwater in sufficient amounts.

CHAPTER ONE

INTRODUCTION

1.1. General

Human life; as with all animal and plant life on the planet; is dependent up on water. Not only do we need water to grow our food, generate our power and run our industry but we also need it as basic part of our daily lives. Our bodies need to ingest water every day to continue functioning. Communities and individuals can exist without many things like shelter, even without food for a period, but they can not be deprived of water and survive for more than a few days. Because of the intimate relationship between water and life, it plays a vital role in the development of community since a reliable supply of water is an essential perquisite for the establishment of a permanent community.

In essence, the degree of utilization of its water resources determines the development level of a country. The use of water both for intensive agricultural and industrial endeavors determines how well the society is using its resources. There has been continued need for the development of water resources in Ethiopia from supplying water for drinking, domestic and livestock uses to their use in agriculture and industrial ventures.

Of all these needs, the supply of safe drinking water to the rural population is one of the immediate demands. Considering the capital required purifying and transporting surface water for domestic supplies, the use of groundwater becomes an attractive alternative in Ethiopian conditions.

In addition to being clean through the natural process of filtration while passing through geologic formations and thus being suitable for domestic consumption, groundwater provides with replenishable and pollution free natural resource. It provides with a clean, safe and continuous supply of water for both human and livestock consumption and

constitutes the largest available source of fresh water that is far greater than that in lakes, reservoirs and streams combined. The search for this supply of water has become vital in areas where the surface supply of drinking water has become scarce.

Dug wells that store water from undeveloped springs and large surface reservoirs of water that fill up during the rainy seasons have become the mainstay of water supply in rural Ethiopia. These supplies, in addition to being susceptible to pollution since they are exposed to external objects falling into them directly or through discharge of domestic and livestock wastes, they also become inadequate in years of dry and minimal rain. The supply of water from these sources has made water borne diseases the main concern of rural health functions. In regard to the seasonal scarcity, rural Ethiopia spends a considerable portion of the working day in search of drinking and home supply water during dry seasons while there is plentiful supply of water, albeit not clean, during the rainy seasons and the few months following it. One of the main means of livelihood in the countryside- the cattle- have to be taken to drinking sites to far off distances and in alternate days and, where the shortages are acute, circumstances may dictate that migrations of a section of the population become common feature.

With abundant supply of surface runoff and percolating water to recharge the subsurface water reservoir during the rainy seasons, there is a plentiful potential supply of clean groundwater in most parts of the country. This being the case, however, rural development programmes and other governmental services have not really concerned themselves with the extraction and supply of this vast water resource.

In this project work we attempt to look for potential sites for the extraction of groundwater for domestic and livestock consumption in a typical area where acute shortage of water during the dry seasons and clean water during the rainy seasons is the main concern. The area chosen is close to Mojo town and on the Mojo-Shenkora road some 80 km from Addis Ababa. Although very rich in agricultural products, the area suffers from sever shortages of water for most part of the year.

The study area is mainly drained by the Mojo River catchments that are dry during summer time and where adequate water supply has always been a problem. The problem in the area is becoming progressively more acute with the growth of the population to around six thousand. To alleviate this problem it was planned to conduct groundwater study in the area that would better determine the groundwater potential of the area and determine highly likely locations for the extraction of water supply to the communities.

Groundwater is any water found below the land surface. It is found in aquifers in the pore spaces of rocks. It flows to the surface naturally at springs and seeps and can form swamps. It may also be tapped artificially by the digging of wells. In Ethiopia Groundwater is occurring in different part of the country within different hydrogeological environment and aquifer settings that is being partly developed for water supply purposes. It is known that most of the water supply sources of the country must be groundwater sources because its morphological setting most part of the country are affected by surface runoff and much work is also expected in future to satisfy the water demand especially in the rural area.

The study area has low groundwater occurrences for a number of boreholes failed; even digging of hand dug wells near their villages is unusually unproductive fetching of water from far sites gives women and children heavy laden as it is in most part of the country. Therefore, the probability of getting groundwater in the area is low, however, owing to the presence of rocks of various formations exposed to variable degree of weathering and fracturing and vertical structures with considerable extension, which could allow the percolation of rainwater (the main groundwater recharge in the area) to deeper formation, groundwater may be expected at depths greater than 80m. (Alem, 2004)

This project work is aimed at exploring for the possibilities for supply of mainly drinking water to the rural communities of Deka Bora and Tulu Rei close to Ejere town. In the area, the main water supply source is traditionally dug well, collecting ponds and spring water that is far from their residence. Sometimes the population fetches drinking water

from Mojo town, 20 km away from their living area. As the community representative and elders reported to us in the discussion, and as we also observed during survey time, the community spends their substantial time in fetching water.

Over the study area there are eight drilled bore holes, but all of them have no water at all. From preliminary studies boreholes drilled at Tulu Rei and Deka Bora have a depth of 220m and 295m respectively, but both were found to be dry. The beneficiaries said that they get water from the hand-dug ponds during the rainy season whereas they take their water consumption from distant areas during dray season. To fulfill the water demand of the households, women and children spend more time in fetching water from ponds or rivers. Therefore, availability of adequate water at a reasonable distance will alleviate the burden of water fetching for this group of society.

From the general geology of the Main Ethiopia Rift (MER), the quaternary, lacustrine and alluvium deposits of the flood plains and valley fills are very important hydrogeologic formations. The Mojo town groundwater sources are also these lacustrine and alluvium deposits; where as in the study area the highly fractured quaternary volcanic (basalt, ignimbrite and rhyolitic ignimbrite) are the main sources. From geological and hydrogeological evidence, the study was conducted to investigate groundwater supply to the communities of Tulu Rei and Deka Bora and alleviate water problem in the area. The above-mentioned dry boreholes have failed probably due to unskilled personal interpretations of the geological investigations or the drilling was carried out without any geological, hydrogeological or geophysical information, but there was no any geophysical work carried out.

To that end, the study used the electrical resistivity methods that consist of various principles and techniques to identify available water in the area. The electrical conductivity of the earth materials can studied by measuring the electrical potential distribution produced at the earth's surface by an electric current that is passed through the earth. In homogeneous subsurface medium it is possible to calculate the potential distribution and the path of the current flow from the knowledge of the electrode

separations and the magnitude of the current applied. However, the presence of a zone with anomalous resistivity, which may be due to discontinuity of rock formation or change in its physical condition, perturbs the distribution of the current or potential line, compared to their pattern in a homogeneous medium. Since, the earths subsurface are not homogeneous; the measured quantity in electrical resistivity method is the apparent resistivity, which is the representative of the ground under investigation.

1.2 Previous Studies

Several researchers have studied the Mojo area for its groundwater potential (Alem, 2004 and the references therein; Tesfaye Chernet et al., 1998). Even if several works were employed in the region particularly, in the study area most of the works focused on geological and hydrogeological studies.

In the area there are eight dry boreholes but around 10 km far from the Deka Bora and Tulu Rei at Gegola Arifta peasant association there is one functional bore hole that discharge 6.6 litters per second with the same geological and hydrogeological situation to this study conducted area.

The annual recharge ranges from 50-150 mm per year in the Mojo and its surrounding (Tesfaye Chernet, 1993). This is due to relatively low rainfall and relatively higher potential evaporation. The region is characterized by localized groundwater with moderate to large quantities particularly along valleys and side of it. From the geoelectricsection of Bermiji near to the study area, Mojo source (JICA, undated); cited in Alem, 2004). The geologic structures are identified. The central zone appears to have been uplifted and it makes the area to have low groundwater occurrence.

1.3 objectives of the project

The main objectives of this research work are:

- Mapping the subsurface geoelectrical layers, for identifying the layers that are capable of storing groundwater.
- Determining the depth of these water bearing horizons, if and where they e

- Mapping the major structure (like faults, fractures, fissures, etc) that may control the movement of groundwater.
- Locate preferred sites for boreholes and their depth in the two communities for the extraction of groundwater.

1.4 Methodology

The particular purpose of this research work is to achieve the objectives set above by applying different geophysical methods. Various geophysical techniques are normally applied for groundwater investigation with some showing more success than others. To achieve these objectives, electrical resistivity and gravity geophysical survey were conducted in this project work but, only electrical resistivity data processed and interpreted.

During the field survey, apparent resistivities (ρ_a) were measured along the proposed line. The traverse lines for the survey were selected to cross possible structures over the area and the gravity and resistivity data were taken along the same line so that they compliment one another in the interpretation. In addition, analysis of the rock and soils of apparent resistivities were performed using measured data. The interpretations were made from the generated geoelectricsection map. Finally, the results are integrated with the available geological information on whose bases conclusions are forwarded regarding the availability of groundwater in the area and the horizons that bear this water.

Accordingly, the next five chapters present a theoretical description, methodology of the fieldworks and field results, including data analysis, presentation and interpretations of the results. A final section presents concluding remarks about the work and some recommendations to follow up the work.

1.5 Instruments and Materials Used

The instruments used during the electrical survey were the 16GL earth resistivity meter and the standard P300 Booster package contains:

- No. 1 energizer model P300
- No. 1 battery charger
- No. 1 cable complete of connector to an external battery
- connecting cables and others accessories

Some of the general characteristics of the instrument are:

High resolution (16 bit and floating point)

High sensitivity (minimum measurable voltage: 610 nV)

Managed by microprocessor

Continuous readout by both current and voltage etc

The important materials and relevant data used were

a. Published and unpublished reports for literature review (Getachew, 2004; Alem, 2004)

b. Topographic maps, with scale of 1:50,000

c. GPS

1.6 General Overview of the Area

1.6.1 Location, Accessibility and Topography

The project area is situated in the Main Ethiopia Rift (MER) at a distance of about 80 km from Addis Ababa on a detour east of Mojo town along the Mojo-Ejere-Shenkora all weather gravel road. The area is found in Mojo district where two Peasant Associations (PA) people lived and lies between $39^{0}00'$ and $39^{0}15'$ East longitude and $8^{0}36'$ and $8^{0}45'$ North latitudes. The area comprises of several villages and numbers of farming communities with approximate total population around 6000 people living in the selected peasant associations. After initial survey and site selection visits, these two peasant

associations of Tulu Rei and Deka Bora were selected for detailed study included in this project work. Climatologically, the area falls in the tropical rainy zone with mean annual rainfall varying from 680 mm to 2000 mm and average temperature of coldest month is 18^0c. A hot summer with maximum temperature ranging from 20.9^0C to 24.7^0C where as the highest temperature is being recorded in May and the lowest in August taken from Mojo town station which is 20km far from the study area.

The topography of the study area and around it comprises of plateau and volcanic piedmonts with extensive faults, hilly and valley land form of the rift margin, and to the south, it extends to the volcanic alluvial and flood plains of the rift valley. The average elevation in the catchments ranges between 1780m to 3100m above mean sea level at Mojo town and mount Yerer respectively.

An adequate water supply, particularly during dry season, has always been problem in the area. The problem is becoming progressively more acute with the growth of population. At present, only Mojo town is provided with piped water supply from the wells.

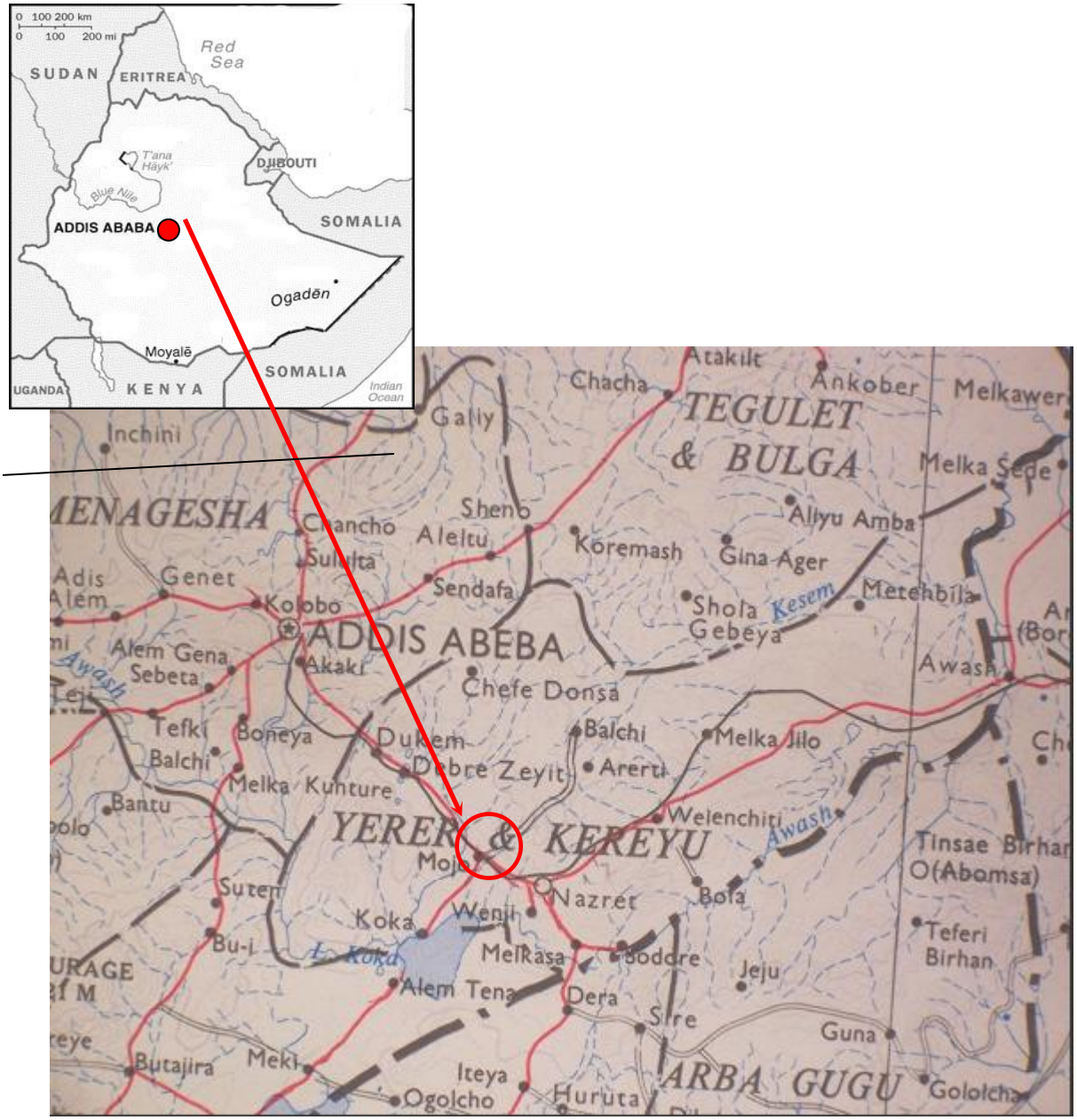

Figure 1 General Location Map of the Study Area

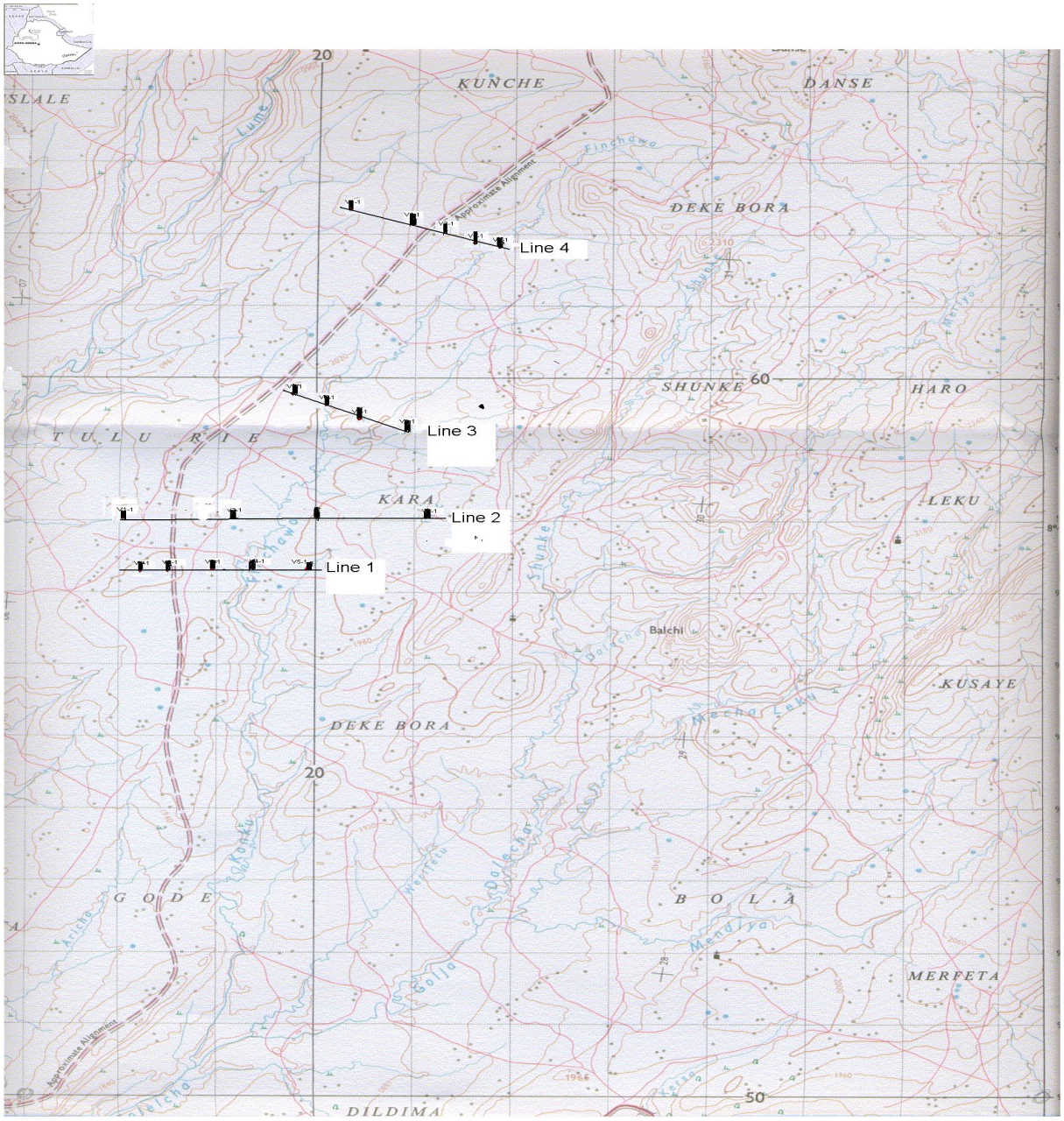

Figure 2 Location Map of the Survey Area and the Sounding Points (detailas of the region marked with circle on Figure 1)

1.6.2 Geology of the study area

In the area the landscapes are further subdivided into different relief forms thus, from fault scarps to gently slopping land forms, where as the volcanic lacustrine plain shows variation in relief form. The Quaternary volcanic rocks comprise of tuft, pumices, ignimbrite pyroclastic flows and different volcanic fragment scoria and basaltic flows. In the single pile of the volcanic tuff deposits two or three different eruption episodes could be easily identified that are separated by development of pailosoil.

A detailed geological mapping of the Debrezeit and Mojo area allowed the recognition of ten volcanic units that were grouped in to four volcanic complexes (Tsegaye Abebe et al., 1999) stratigraphic relationships between the recognized units have been further constrained by new K-Ar measurements. The volcanic complexes define three main structural sectors. These are

- The western rift margin
- The Main rift floor
- Intra-rift depression

The western rift margin included the Addis Ababa ignimbrite that constituted by different flow units, consisting pale green to pal yellow welded and crystal rich comenditic and patelleritic ignimbrites, constitute the sequences. Two K-Ar age determinations (Tesfaye Chernet et al., 1998) have given ages of 5.1 and 3.3 My respectively.

In this margin central volcano that includes Yerer volcano and products of the composite volcanoes of Wechacha and Furi are present. Among them it is Yerer volcano unit, which out crops in the study area and it dates back 3.9-3.3My according to new K-Ar dating.

The intra- rift depression consists of the Nazareth unit that constitute the upper part of Nazareth group of Kazmin and Seifemichael Berhe (1979) with respect to age

constraints this unit lasted about 2My, from 3.1 to 5.4 My (Tsegaye Abebe 1999). Basically tow types of ignimbrite (top) have been identified: the slightly welded ignimbrite (bottom), separated by paleosoil and lacustrine deposits.

Tulu Rie Basalt crops out in the eastern and northern section of the study area and it belongs to intra rift complex where it covers the Nazareth unit and forms the upper of NE trending escarpments. The age ranges between 8- 2.7 My. The Tulu Rie Basalt is considered, for its stratigraphic positions and compositions as a part of Bofa basalt. Chefe Donsa unit also belongs to intra-rift complex. The volcanic rocks of Chefe Donsa unit are exposed mainly along the border of the central plain. They consist of all deposits and poorly wielded ignimbrites of rhyolitic compositions. They are fairly distributed in the Mojo river catchments. It covers the Nazareth, Tulu Rie basalt and Yerer product.

The Bishoftu volcanic unit is belongs to the main rift floor and forms NNE trending belt outcropping mainly in the central flat area of Mojo river catchments. It indicates the most recent basic products of the Debrezeit areas, (Tsegaye Abebe et al., 1999) which coincides with the name younger volcanic by (Grasparon et al., 1993). In Bishoftu volcanic there are two groups represented by spatter and cinder cones with associated tabular lavas and phreatomagmatic deposits respectively. The latter, consisting mainly highly fragmented deposits are chiefly concentrated in the central part, where the highest thickness of the lacustrine sediments frequently intercalated with the phreatomagmatic products. The composition of lavas and juvenile glass ranges from alkalic basalts to olivine basalts to trshyandesists (Tsegaye Abebe et al., 1999).

Vascular basalt is found associated with and or sandwiched between pyroclastic and lacustrine deposit and covering the volcanic tuffs in some parts of the area. It is dark gray in color, vascular, massive and sometimes scoracious and at places secondary precipitates, dominantly, zeolite sand calcite fills the vesicles.

Lacustrine deposits and alluvial cover of the study area, the quaternary sediments are composed of fluvo-lacustrine deposits of alluvium, colluvium, elluvium, coarse sand,

salty sand and siltstone. Mojo and its surrounding areas are supposed to have been covered by ancestral lake during the pluvial period of quaternary. The lacustrine sedimentation are the results of deposition in this large ancestral lake (Mohr, 1967; and Tsegye Abebe et al,1999).The lacustrine beds are inter bedded volcanic sands, siltstone sandstone, calcareous materials and diatomite with intercalation of water-laid tuffs. The sandy and silt sand deposits are layered horizontally with graded bedding and cross lamination. They are very friable, less compact and hammered very easily .The late quaternary rocks were deposited alternating with the volcanic tuffs and pumice .The deposited volcanic sands and associated sedimentary rocks fine grained and or connected by fine grained materials.

Tectonic and structures of the study area, Mojo like the other rift valley areas was subjected to tectonic activities and intense volcanism. Some faults have been observed in this area forming minor fault escarpment. The river channels, large gullies seem to outline and follow the hidden and an exposed fault line. In the main Ethiopian rift valley, faults, joints, fractures, volcanic flows and layering and flow fold in, which are associated with silica lava flows are main geologic structures. The presence of thick fluvo-lacustrine deposits and active erosion or denudation process in the MER during the fluvial period of the Quaternary mask the probable existence of fault/lineaments.

Brittle deformation consisting of fractures, joints and faults are dominant in the area. Structures are extensional and affected chiefly the rocks of the intra rift complex and partially those of the western rift margin complex. These structures are grouped into four main fracture systems consisting mainly of joints sets and some faults (Abebe et al., 1999).Those are the N-S/NNE-SSW fracture system which is an analogous to Wonji fault belt, constitute normal faults with steeply dipping joints dip angle of grater than 85^{o}.The next one is NE-SW fracture system that parallels the regional trend of the MER, and has normal fault of 1m thrown and dip angle greater than 85^{0}. It is wide spread especially in the Nazareth unit where the most important physiographic features are NE ridges and escarpments

The third one E-W fracture system mainly concentrated in zones close to the Yarer volcano or just east of Addis Ababa. It parallels the trend of the Yerer-Tulu Welel volcanic liniments structures. It consists of sub vertical to vertical joints with dip angle greater than 85^0. The last one is NW-SE fracture system. Few high angle normal faults have been observed with high morphologic evidence. This system affects mainly the oldest unit of western rift margin.

The geology of the area is strongly conditioned by the interaction between the left lateral oblique rifting of the MER (Boccallitti et al., 1999) and right lateral transetensional Yerer-Tulu Welel volcanic lineament structure (Tsegaye Abebe et al., 1998).Thus, the interference between the MER and Yarer Tulu Welel volcanic lineament structures would be the first order cause of fractures like gradual transition between the rift floor and the west rift shoulder.

1.6.3 Hydrogeology of the study area

Hydro geological characteristics of litho-logical units of the study area discussed as below

Trachyte lavas, massive ignimbrite lacustrine deposits: In the study area a very small portion area has massive exposure of Addis Ababa ignimbrite that it has poor hydraulic conductivity. Lacustrine sediments cover most of the northwestern part of Mojo town. The thickness increases from northwest to southeast. The thickness increases from northwest to southeast. These sediments are exposed in the study area with thin but extensive spatial distribution and consist of sand, silts, clays, tuffs, pumice, and ignimbrite. These sediments, in most places are mixed compositionally with quaternary volcanic products and form a specific mixed volcano-sedimentary rock type. Lacustrine deposits are exposed at the surface of the study area they appeared to be a loosely cemented material texturally ranging from fine grained to coarse grained. Tuff, diatomite and ignimbrite are partially interbedded in the lacustrine sediments and at some places

form and extensive layers. Therefore, the permeability of this aquifer unit is some how reduced due to the intercalation of tuff layers.

Fractured ignimbrite and rhyolitic ignimbrite: The ignimbrite and rhyolitic ignimbrite cover most part of the study area. From visual observation in most cases the ignimbrites area well jointed and faulted. These faults and joints can serve as an important groundwater recharging conduit in the absence of secondary filling material.

The rhyolitic ignimbrite in the study area shows a bit difference from the non-rhyolitic ignimbrite by their well-welded nature and by having fractures and joints in more geometrically order fashion. Joints like columnar basalt area also common but this joints form more of a rectangular shape rather unlike the basalts that shown joints with hexagonal shape.

The other difference is the rhyolitic ignimbrite unit shows a laminar structure, which may give a chance for development of fractures and easy for groundwater circulation.

Alluvial and basaltic flows and domes: The alluvial cover mainly out crop above the products of the western rift margin complex and consists of regolith, and alluvium with maximum thickness about 2m. Basaltic lava flows that are found in the eastern and southern part of the study area are scattered in the form of younger spatter and cone volcanic centers. These basalts are highly fractured and in several places they are scoraceous. Therefore, they have high permeability and productivity.

CHAPTER TWO

GEOPHYSICAL SURVEYS

2.1 General

Geophysical surveys greatly help in studying the groundwater potential in any hydrogeological setup and locate preferred borehole locations and determine the depth to the aquifers. The property and thickness of various lithological units obtained from geophysical survey at different location has been given much attention in part by a desire to reduce the risk of drilling dry holes and also a desire to offset the cost associated with poor ground in groundwater. However, geophysical surveys are not always the most effective method of obtaining the information needed. Fore example, in some areas drill holes may be a more effective way of obtaining near-surface information than geophysical surveys. In some investigations a combination of drilling and geophysical measurements may provide the optimum cost benefit ratio.

In general, geophysical surveys are not practical in all groundwater investigations, but this determination usually can be made only by someone with an understanding of the capabilities, limitations, and costs of geophysical surveys. A clear definition of the geologic or hydrogeologic problem and objectives of an investigation is important in determining whether exploration geophysics should be used or not. The lack of a clear definition of the problem can result in ineffective use of geophysical methods.

In the study area, the hydrogeological characterization of different volcanic and sedimentary products in Mojo river catchments was largely done by using the visual observation of the formation as well as referring different geological surveys conducted prior to the geophysical surveys. Quaternary volcanic are young volcanic of the Maine Ethiopian Rift floor where high tectonic activity is occurring which has resulted highly fractured rocks and as a result a favorable situation for groundwater recharge and occurrence exist (Getachew, 2004).

Based on the above condition and past geological and hydrogeological information (Alem, 2004), it was decided to conduct an electrical resistivity Vertical Electrical Sounding (VES) survey to supplement the geological and hydrogeological investigations conducted over the project area and also to provide additional subsurface information about the lithologic units and major structures that may control the circulation and movement of groundwater.

2.2 Electrical Resistivity Methods

The electrical properties of most rocks in the upper part of the earth's crust are dependent primarily up on the amount of water in the rock, the salinity of the water, and the distribution of the water in the rock. Saturated rocks have lower resistivities than unsaturated and dry rocks. The higher the porosity of the saturated rock, the lower its resistivity, and the higher the salinity of the saturating fluid, the lower the resistivity, whiles the presence of clays and conductive minerals also reduce the resistivity of the rock.

Two properties of primary concern in the application of electrical methods are the ability of rocks to conduct an electric current, and the polarization that occurs when an electric current is passed through them. The electrical conductivity of earth materials can be studied by measuring the electrical potential distribution produced at the earth's surface by an electric current that is passed through the earth or by detecting the electromagnetic field produced by an alternating electric current that is introduced in to the earth.

In this research work electrical resistivity method particularly Vertical Electrical Sounding (VES) was employed, which provides quantitative depth information below ground level of the individual layers. The method has found the greatest application to groundwater because of its high resolving power with respect to vertical stratification and delineating saturated zones.

Direct Current Resistivity Method

In the period from 1912 to 1914 Conrad Schlumberger began his pioneering studies which lead to an understanding of the merits of utilizing electrical resistivity methods for exploring the subsurface (Dobrin, 1960). According to Breusse (1963), the real progress in applying electrical methods to groundwater exploration began during world war II. French, Russian and German geophysicists were mainly responsible for the development of the theory and practice of direct current electrical prospecting methods.

The resistivity of rocks and minerals displays a wide range. No other physical property of naturally occurring rocks or soils displays such a wide rang of values. In most rocks, electricity is conducted electrolytically by the interstitial fluid and resistivity is controlled more by porosity, water content, and water quality than by the resistivities of rock matrix. Clay minerals, however, are capable of conducting of electricity electronically, and the flow of current in a clay layer is both electronic and electrolytic.

2.2.1 Basic Principles of the Resistivity in Homogeneous Earth

In the resistivity method an electric current is introduced in to the ground by means of two current electrodes, and the potential difference between two pair of potential electrodes is measured. The potential difference between two arbitrary located points on the surface of a homogeneous isotropic ground is can be derived as follow.

The flow of current in a medium is based on a principle of conservation of charge and is expressed by relation

$$(I_c)_s = - \frac{dQ}{dt} \qquad (1)$$

where I_c is the current flowing out of a closed surface's' and Q is the charge enclosed by s. In terms of current density J and charge density q, $(I_c)_s$ and Q are given by

$$(I_c)_s = \oint j ds \tag{2}$$

$$Q = \int v\, q\, dV \tag{3}$$

where v is the volume bounded by the surface s. By substituting equation (2) and (3) in to (1) one can develop the formula

$$\oint_s j ds = \int v\, q\, dV \tag{4}$$

Using the divergence theorem

$$\oint j\, dq = \int v (\nabla . j) dV \tag{5}$$

And interchanging the differentiation and integration sequence

$$\int_v (\nabla . j)\, dV = -\int_v \frac{\partial q}{\partial t} dV \tag{6}$$

or

$$\int_v \left(\nabla . j + \frac{\partial q}{\partial t} \right) dV = 0 \tag{7}$$

since the volume used is arbitrary, equation (7) must hold for

$$\nabla . j + \frac{\partial q}{\partial t} = 0 \tag{8}$$

or

$$\nabla . j - \frac{\partial q}{\partial t} \tag{9}$$

This relation is known as equation of continuity. For stationary current

$$\frac{\partial q}{\partial t} = 0$$

Then equation (8) reduce to

$$\text{Div } J = 0 \qquad (10)$$

Since the electric field, $\mathbf{E}$, is conservative field it may be related to the scalar function V (potential) as

$$\mathbf{E} = -\nabla . V \qquad (11)$$

if ρ is the resistivity of the medium, hence the current density J is related to the electric field intensity **E** by means of Ohm's law which is given as

$$J = \frac{1}{\rho}\mathbf{E} = -\frac{1}{\rho}\,\text{grad } V \qquad (12)$$

where V is the electric potential. For an isotropic medium, ρ is a scalar function of the point of observation and J is in the same direction as $\mathbf{E}$.

For an isotropic medium, we get from relations (10) and (12)

$$div\left(\frac{1}{\rho} grad\, V\right) = 0 \qquad (13)$$

$$grad\left(\frac{1}{\rho}\right) grad\, V + \frac{1}{\rho} div\, grad\, V = 0 \qquad (14)$$

This is the fundamental equation of electrical prospecting with direct current. If the medium is homogeneous, ρ is independent of the coordinate axes and equation (14) reduce to

$$\text{div grad } V = 0$$

$$\nabla^2 V = 0 \qquad (15)$$

Thus, the electric potential distribution for direct current flow in a homogeneous isotropic medium satisfies Lap lace's equation.

Let us now suppose that a current I be introduced into an infinite homogeneous medium at a point p. Then the potential at a distance r from p will be a function of r and hence Lap lace equation can be written as

$$\frac{d^2V}{dr^2} + \frac{2}{r}\frac{dV}{dr} = 0 \qquad (16)$$

Current is introduced into the ground by means of two electrodes, i.e., a source and sink; and the potential at any point due to this " bipolar" arrangement is

$$V = \frac{1\rho}{2\pi}\left(\frac{1}{r_1} - \frac{1}{r_2}\right) \qquad (17)$$

where r_1 and r_2 are the distances of the point p from the source and the sink, respectively.

Consider that a direct current of strength I is introduced into a homogeneous and isotropic earth by means of tow point electrodes A and B (Figure 1). The potential difference between the tow points M and N on the surface is given by using equation (16) as

$$\left(\frac{1}{AM} - \frac{1}{AN}\right) - \frac{1}{BM} + \frac{1}{BN}$$
$$\Delta V = \frac{I\rho}{2\pi}\left\{\left(\frac{1}{AM} - \frac{1}{BM}\right) - \left(\frac{1}{AN} - \frac{1}{BN}\right)\right\} \qquad (18)$$

where ρ is the resistivity of the ground thus, the resistivity of the homogeneous earth can be determined from the measurement on the surface.

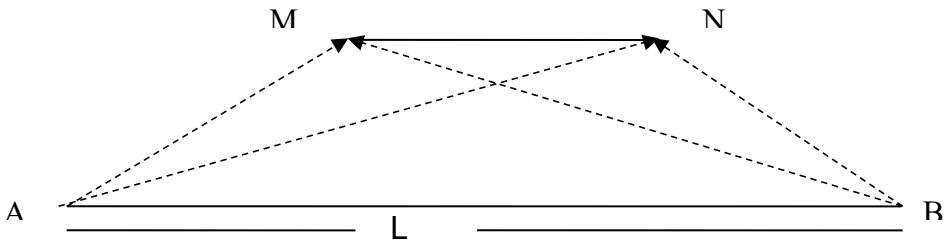

Figure 3a point electrodes over a homogeneous and isotropic earth. (AB -point source and sink; MN - observation points on the surface of the earth)

Various electrode arrangements for A, B, M and N have been suggested for the purpose. The ones more commonly used for resistivity sounding are: symmetrical arrangement and dipole arrangement.

In the symmetrical arrangement, the points A, M, N, and B are taken on a straight line such that the points M and N are symmetrically placed about the center 0 of the "spread" AB (Figure 3)

Another basic physical concept in any geophysical prospecting is depth investigation. Roy and Apparao (1970) defined the depth of investigation in any direct current resistivity method as that depth at which a thin horizontal layer contributes the maximum amount of the total measured signal at the ground surface.

The depth of investigation has been considered synonymous with the depth of current penetration or their distribution; but a current distribution of penetration is a function of

only the position of the current electrodes where as the depth of investigation is determined by the position of the potential and current electrodes.

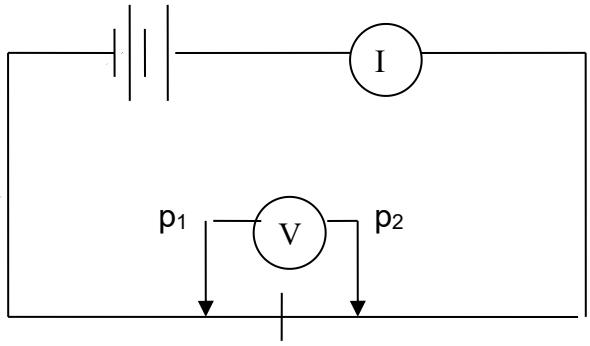

Figure 3b The Schlumberger symmetrical electrode arrangement.

Here $$V_{P1} = \frac{1\rho}{2\pi}\left(\frac{1}{r_1} - \frac{1}{r_2}\right)$$

$$V_{p_2} = \frac{1\rho}{2\pi}\left(\frac{1}{r_3} - \frac{1}{r_4}\right)$$

$$\Delta V = V_{p_1} - V_{p_2} \tag{18}$$

$$\Delta V = \frac{1\rho}{2\pi}\left(\frac{1}{r_1} - \frac{1}{r_2} - \frac{1}{r_3} + \frac{1}{r_4}\right)$$

$$\frac{1}{k} = \frac{1}{2\pi}\left(\frac{1}{r_1} - \frac{1}{r_2} - \frac{1}{r_3} + \frac{1}{r_4}\right) \tag{19}$$

which gives $$\rho_a = K\frac{\Delta V}{I} \tag{20}$$

In the Schlumberger arrangement, $L \geq 5b$, we can put $(L^2 - b^2)$ in equation (19) equal to L^2 with an error less than 4%. In this case, the resistivity is given by:

$$\Delta V = \frac{I\rho}{2\pi}\left[\frac{2b}{L^2} - b^2\right] \tag{21}$$

$$\rho_a = 2\pi\left[L^2 - \frac{b^2}{2b}\right]\left(\frac{\Delta V}{I}\right)$$

$$K = 2\pi\left[L^2 - \frac{b^2}{2b}\right]$$

$$\rho_a = k\frac{\Delta V}{I} \tag{22}$$

Apparent Resistivity: Using the formulae given so far, we can find out the resistivity of a semi-infinite homogeneous earth by means of symmetrical arrangements discussed earlier. For an inhomogeneous medium we define a quantity ρ_a, known as the apparent resistivity. The apparent resistivity of a geological formation is equal to the true resistivity of a fictitious homogeneous and isotropic medium in which, for a given electrode arrangement and current strength I, the measured potential difference V is equal to that for the given inhomogeneous medium. The apparent resistivity depends upon the geometry of the electrode arrangements and the resistivities of the elements constituting the given geologic medium. Thus;

$$\rho_a = k\left(\frac{\Delta V}{I}\right)$$

Broadly speaking, we can distinguish two types of resistivity measurements. In the first, known as geoelectric profiling or mapping, the value of k remains constant for a particular set of readings, and measurements are done at various points on the surface. In this way, we get the surface lateralvariation of apparent resistivity values within a certain depth. In the second method, known as geoelectric soundings, for a particular

set of readings the measurements are done at a specified point such that the value of k progressively changes. In this way, the apparent resistivity values at the surface reflect vertical distribution of resistivity values in a geologic section. This is why geoelectric sounding is some times known as "vertical electrical drilling".

An arrangement of electrodes which is widely used is the symmetrical ones, where current electrodes A, B are symmetrically placed with respect to the potential electrodes M, N (Figure 2), and where the center of the spread, 0, is the sounding point. In the Schlumberger method, the sounding may be done by moving only the current electrodes, progressively increasing the distance AB. However when AB is very large compared to MN, the potential difference between M and N may be too small to be measured with sufficient accuracy. Hence, in practice it is necessary also to increase the distance between N and M, whenever required, depending on the sensitivity of the measuring instrument. The value of MN and the corresponding values of AB are chosen in order to get overlapping readings whenever a change over of MN from one value to the other takes place.

2.2.2 Resistivity Sounding Principle in Horizontal Stratified Earth

In electrical prospecting it is often necessary to determine the depth and the electrical resistivity of a series of horizontal or nearly horizontal stratified ground. In order to solve this problem, we should calculate the potential and the electric field, due to a point source of current, at any point on the surface of a stratified earth. This has advantages because it enables one to use the axial symmetry of the potential field about the vertical axis through the current source and the additive ness of the potential is also be used.

Let us choose a cylindrical system of coordinates, with the origin at the point source a direct current located on the surface. The subsurface consists of infinite number of layers separated by horizontal boundary planes, the deepest layer existing to infinite depth ($h_n \to \infty$) and the other layers have finite thickness h_i = h_1, h_2, h_3 .....h_n and resistivities $\rho_1,\rho_2,.....\rho_n$. Each of the layers is electrically homogeneous and isotropic. The derivation of the potential based on the above conditions was first due to Steanescu et. al.,(1930).

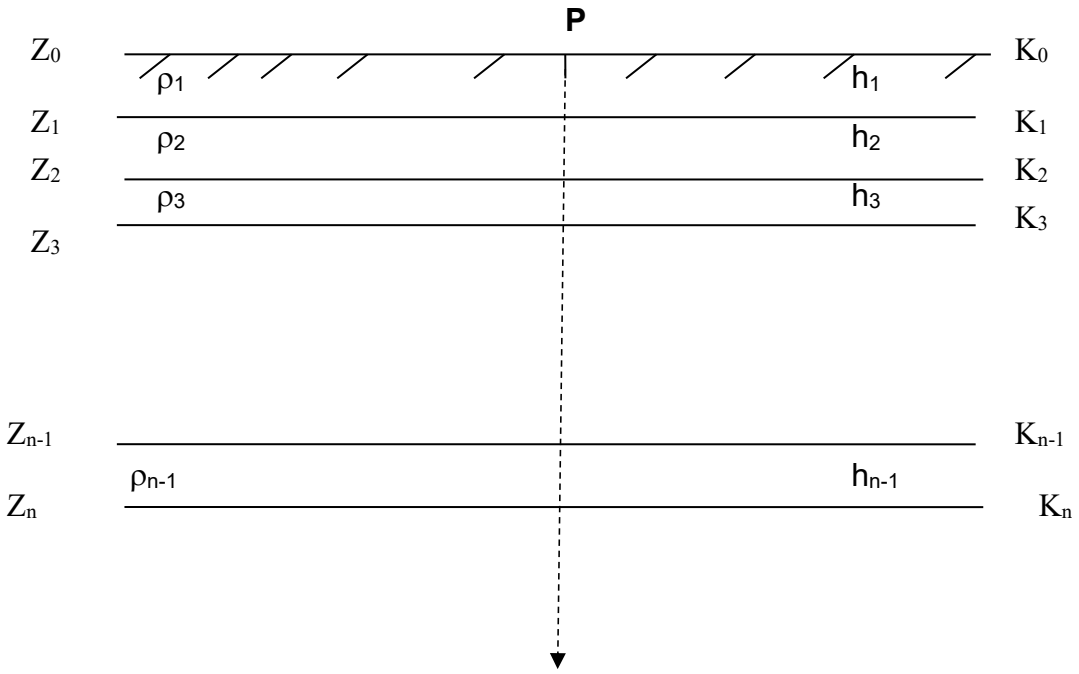

Figure 4. A multi-layer earth and problem presentation for solution of the potential

The electrical potential field V, for direct current satisfies the differential equation of Laplace, which is

$$\nabla^2 V = 0$$
$$or \frac{\partial^2 V}{\partial x^2} + \frac{\partial^2 y}{\partial y^2} + \frac{\partial^2 V}{\partial z^2} = 0 \quad (23)$$

The potential field has a cylindrical symmetry with respect to the vertical axis line through the current source. Therefore, Laplace equation in cylindrical coordinate will be

$$or \frac{\partial^2 V}{\partial r^2} + \frac{1}{r}\frac{\partial V}{\partial r} + \frac{\partial^2 V}{\partial z^2} = 0 \quad (24)$$

For a solution symmetrical with respect to the vertical axis $dV/d\theta$ and $d^2V/d\theta^2=0$, so that

$$or \frac{\partial^2 V}{\partial r^2} + \frac{1}{r}\frac{\partial V}{\partial r} + \frac{\partial^2 V}{\partial z^2} + \frac{1}{r^2}\frac{\partial^2 V}{\partial \theta^2} = 0 \quad (25)$$

The particular solution of equation (24) can be obtained using the method of separation of variables, and can be assumed to be of the form

$$V(r,z) = U(r)\ W(z) \quad (26)$$

substituting equation (25) to (24) and dividing throughout by the product U(r) W(z) gives

$$\frac{1}{U(r)}\left(\frac{d^2U(r)}{dr^2}\right) + \frac{1}{rU(r)} \qquad \frac{dU(r)}{dr} = 0 \quad (27)$$

this equation is satisfied if only if

$$\frac{1}{U(r)}\frac{d^2U(r)}{dr^2} = \lambda^2 \quad (28)$$

and

$$\frac{1}{W(z)}\frac{d^2W(z)}{dz^2} = 0 \quad (29)$$

where λ is an arbitrary constant

The solution of equation (29) may be given as

$$W = Ce^{-\lambda z} \; and \; W = Ce^{+\lambda z} \tag{30}$$

and that of equation (28) is given as

$$U(r) = cj_0(\lambda r) \tag{31}$$

where J_0 is the Bessel function of order zero

The combination of equation (30) and (31) gives the particular solution of the deferential equation given by equation (25), which is

$$V = ce^{-\lambda z} j_0(\lambda r)$$

and

$$V = ce^{+\lambda z} j_0(\lambda r) \tag{32}$$

where c and λ are both constants in the last of these equations.

Since, by theory of differential equations, every linear combination of the particular solution is also a solution, one can make λ to rough all possible values from 0 to ∞ and allowing the constant "C" to very independence of λ, the general solution of equation (25) can be obtained as

$$V = \int_0^{\infty} \left[\phi(\lambda) e^{-\lambda z} + \chi(\lambda) e^{+\lambda z} \right] j_0(\lambda r) \, d\lambda \tag{33}$$

Here Φ (λ) and χ(λ) are arbitrary functions of λ. The boundary conditions control the special form of these equations

From the basics theory, the potential generated by a single point source of current intensity I located at the surface of an electrically homogeneous earth is given by

$$V = \frac{I\rho}{2\pi} \qquad \left(\frac{1}{\sqrt{r^2 + z^2}} \right) \tag{34}$$

where ρ is the resistivity of the homogeneous earth.

Equation (34) can be written in integral form by using the so-called Lipschitz Integral (also called the Weber Integral Formula) in theory of Bessel functions as

$$\int_o^\infty e^{-\lambda z} \left(\lambda r \right) d\lambda = \frac{1}{\sqrt{r^2 + z^2}} \tag{35}$$

so that equation (34) gives

$$V = \frac{I\rho}{2\pi} \qquad \int_o^\infty e^{-\lambda z} \; j_o \left(\lambda r \right) d\lambda \tag{36}$$

Equation (36) is also a solution of equation (25). Therefore, the combined solution will also be a solution to the equation, that is

$$V = \frac{I\rho}{2\pi} \qquad \int_o^\infty \left(e^{-\lambda z} + \theta(\lambda) e^{-\lambda z} + \chi(\lambda) e^{-\lambda z} \right) j_o(\lambda r) d\lambda \tag{37}$$

where $\theta(\lambda)$ and $\chi(\lambda)$ are arbitrary function λ. solution of equation (37) are valid in all the layers of the subsurface.

The function $\theta(\lambda)$ and $\chi(\lambda)$ are not, however, necessarily the same in the different layers of the subsurface. Therefore, the potential due to a point source of current at the surface of a horizontally layered earth must in each layer satisfy

$$V_i = \frac{I\rho}{2\pi}\int_o^\infty \left(e^{-\lambda z} + \theta_i(\lambda)e^{-\lambda z} + \chi_i(\lambda)e^{-\lambda z}\right) j_o(\lambda r)\, d\lambda \tag{38}$$

This equation is called the Stefanescu Integral, with i referring to the several layers of the subsurface.

Boundary Conditions

For a potential set up by a single source of current at the surface of a horizontally stratified earth

1) At each of boundary planes in the subsurface the electrical potential must be continuous

$V_i = V_{i+1}$ at $z=h_i$ (39)

2) The vertical component of the current density must be continuous on each boundary plane (the current density normal to the boundary planes)

$(J_i) = (J_{i+1})$

$$\frac{1}{\rho_i}\frac{\partial V_i}{\partial z} = \frac{1}{\rho_{i+1}}\frac{\partial V_{i+1}}{\partial z} \tag{40}$$

3) At the surface (z =0) the vertical component of the current density J_N (and hence that of the electric field intensity) must be zero, everywhere except in the infinitesimal neighbourhood around the current source (in air $J_{air} = 0$ and from condition 2, the vertical component of the current density at depth zero must be zero).

4) Near the current source the potential (v must be finite) must not approach infinity as

$$V = \frac{I\rho}{2\pi} \frac{1}{\sqrt{r^2 + z^2}} \tag{41}$$

5) At infinite depth, the potential must approach zero, that is

$V \rightarrow 0$ as $z \rightarrow \infty$

Application of the Boundary Conditions

1) According to this condition

$$V_i = V_{i+1} \qquad at\ h_i = z$$

$$\int_o^\infty \left(e^{-\lambda h_i} \theta_i(\lambda) e^{-\lambda h_i} + \chi_i(\lambda) e^{+\lambda h_i} \right) j_o(\lambda r) d\lambda$$

$$= \int_o^\infty \left(e^{-\lambda h_i} + \theta_i + 1(\lambda) e^{-\lambda h_i} \right) j_o(\lambda r) d\lambda \tag{42}$$

This equation can be satisfied for all the values of λ if the integrands on both sides are equal, that is

$$\theta_i(\lambda) e^{-\lambda h_i} + \chi_i(\lambda) e^{+\lambda h_i} = \theta_i + 1(\lambda) e^{-\lambda h_i} + \chi_{i+1}(\lambda) e^{+\lambda h_i} \tag{43}$$

2) according to the second condition

$$\frac{1}{\rho_i} \frac{\partial V_i}{\partial z} = \frac{1}{\rho_{i+1}} \frac{\partial V_{i+1}}{\partial z}$$

from equation (16)

$$\frac{1}{\rho_i}\int_o^\infty \left[(1+\theta_i(\lambda))e^{-\lambda h_i} + \chi_i(\lambda)e^{+\lambda h_i}\right] j_o(\lambda r)\, d\lambda =$$

$$\frac{1}{\rho_{i+1}}\int_o^\infty \left[1+\theta_{i+1}(\lambda)e^{-\lambda h_i} + \chi_{i+1}(\lambda)e^{+\lambda h_i}\right] j_o(\lambda r)\, d\lambda \Leftrightarrow$$

$$\frac{1}{\rho_i}\int_o^\infty \left[\left(1+\theta_i(\lambda)\right)e^{-\lambda h_i} + \chi_i(\lambda)e^{+\lambda h_i}\right] =$$

$$\frac{1}{\rho_{i+1}}\int_o^\infty \left[1+\theta_{i+1}(\lambda)e^{-\lambda h_i} + \chi_{i+1}(\lambda)e^{+\lambda h_i}\right] \qquad (44)$$

1) Due to condition three

To satisfy condition 3 first differentiate expression (38) with respect to z and then evaluate its value at z=0 to get

$$\frac{I\rho}{2\pi}\int_o^\infty \left[-1-\theta_i(\lambda)+\chi_i(\lambda)\right] j_0(\lambda r)\, d\lambda = 0 \qquad (45)$$

The first term of this integrand represents the field that would exist in homogeneous earth and is referred to as the primary field (it automatically satisfies the boundary condition).

The last two terms of the integrand together define the perturbed field. The vertical component of the field intensity of the perturbing field must be zero at the surface for all values of r including that at the origin (where the point source of current is located). This condition is satisfied if and only if

$$\theta_i(\lambda) = \chi_i(\lambda) \qquad (46)$$

2) Condition 4

This condition is automatically satisfied by the expression for the primary potential, that is

$$V = \frac{I\rho}{2\pi} \qquad \int_o^\infty e^{-\lambda z}\ j_o(\lambda r)\, d\lambda$$

only by making sure that the perturbing potential remains finite at the origin that is

$$\theta_i(\lambda) = \chi_i(\lambda)$$

3) Condition 5

This condition requires that in the deepest layer (subscript n) the function χ must be zero which has a factor +λz attached to it (this factor will drive the potential to an infinite value at infinite depth). This condition is satisfied with

$$\chi_i(\lambda) = 0 \tag{47}$$

The set of equations (43) to (47) provide a system of equations in unknown function θ(λ) and χ(λ). Such a system can, in principle, be solved.

However, consider the solution of the system for $\theta_i(\lambda) = \chi_i(\lambda)$ which according to equation (46) defines the potential in the first layer (including the surface where the measurements are mead). To obtain the solution for the first layer, substitute equation (46) into equations (43) and (44) and then equation (47) in to the last of equation (43) and (44).

Introduce first the notations

$$U_i = e^{-\lambda h_i}$$

$$V_i = \frac{1}{u_i} = e^{+\lambda h_i} \tag{48}$$

$$and \qquad p_i = \frac{\rho_i}{\rho_{i+1}}$$

from equation (43) for i = 1

$$\theta_1(\lambda)e^{-\lambda h_1} + \chi_1(\lambda)e^{+\lambda h_1} = \theta_2(\lambda)e^{-\lambda h_2} + \chi_2(\lambda)e^{+\lambda h_2}$$

using the notations

$$\theta_1 U_1 + \chi_1 V_1 = \theta_2 U_2 + \chi_2 V_2$$

using equation (44)

$$\theta_1(\lambda) = \chi_1(\lambda)$$

$$(U_1 + U_2)\theta_1 - U_1\theta_2 + V_1\chi_2 = 0 \tag{49}$$

from equation (44) for i =1

$$\frac{1}{\rho_1}\left[(1+\theta_1(\lambda))e^{-\lambda h_1} + \chi_1(\lambda)e^{+\lambda h_1}\right] = \frac{1}{\rho_2}\left[1+\theta_2(\lambda)e^{-\lambda h_1} + \chi_2(\lambda)e^{+\lambda h_1}\right]$$

$$for \qquad \theta_1 = \chi_1$$

$$\frac{1}{\rho_1}\left[(1+\theta_1)e^{-\lambda h_1} + \chi_1 e^{+\lambda h_1}\right] = \frac{1}{\rho_2}\left[1+\theta_2 e^{-\lambda h_1} + \chi_2 e^{+\lambda h_1}\right]$$

$$\frac{1}{\rho_1}\left[(1+\theta_1)U_1 - \theta_1 V_1\right] = \frac{1}{\rho_2}\left[(1+\theta_2 U_1 - \chi_2 V_1\right]$$

$$\theta_1 U_1 - \theta_1 V_1 = \frac{\rho_1}{\rho_2}\left[\theta_2 U_1 - \chi_2 V_1 + U_1\right]$$

$$(V_1 - U_1)\theta_1 + P_1U_1\theta_2 - P_1V_1\chi_1 = (1-P_1)U_1 \quad (50)$$

for i =2 using equation (47)

$$U_2\theta_2 + V_2\chi_2 - U_2\theta_3 - V_2\chi_3 = 0 \quad (51)$$

from equation (44) for i =2

$$-U_2\theta_2 + V_2\chi_2 + p_2U_2\theta_3 - p_2V_2\chi_3 = (1-p_2)U_2 \quad (52)$$

For i= n-1 equation (43) (using also $\chi_n = 0$ equation (45)

$$U_{n-1}\theta_{n-1} + V_{n-1}\chi_{n-1}\theta_{n-1} = 0 \quad (53)$$

from equation (44) for i =n-1 and $\chi_n = 0$

$$-U_{n-1}\theta_{n-1} + V_{n-1}\chi_{n-1} + p_{n-1}U_{n-1}\theta_{n-1} - p_{n-1}V_{n-1}\chi_{n-1} = (1-p_{n-1})U_{n-1}.$$

The solution of this system of equations for θ_1 is obtained by CRAMER'S rule. According to this rule, θ_1 is obtained as a quotient of two determinants. The denominator is the determinant of the matrix that is formed by the coefficients of θ and χ on the left hand side of the equations of the system.

The equations obtained are

$$(U_1 + U_2)\theta_1 - U_1\theta_2 + V_1\chi_2 = 0 \quad (49)$$

$$\theta_1(V_1 - U_1)\theta_1 + p_1U_1\theta_2 - p_1V_1\chi_1 = (\lambda - p_1)U_1 \quad (50)$$

$$U_2\theta_2 + V_2\chi_2 - U_2\theta_3 - V_2\chi_3 = 0 \quad (51)$$

$-U_2\theta_2 + V_2\chi_2 + P_2U_2\theta_3 - p_2V_2\chi_3 = (\lambda - p_2)U_2$ (52)

$U_{n-1}\theta_{n-1} + V_{n-1}\chi_{n-1} - U_{n-1}\theta_{n-1} = 0$ (53)

$-U_{n-1}\theta_{n-1} + V_{n-1}\chi_{n-1} + p_{n-1}U_{n-1}\theta_{n-1} - p_{n-1}V_{n-1}\chi_{n-1} = (\lambda - p_{n-1})U_{n-1}$ (54)

similar expression could be obtained for the terms letting i =3 , 4..... n-2 to get the equations in the middle of this set.

The Kernel function and its relation to subsurface parameters

$\theta_1(\lambda) = \chi_1(\lambda)$ and z = 0, equation (37)

$$V_i = \frac{I\rho}{2\pi}\int_o^\infty \left(e^{-\lambda z} + \theta_i(\lambda)e^{-\lambda z} + \chi_i(\lambda)e^{-\lambda z}\right) j_o(\lambda r)\, d\lambda$$

The Stefanescu Integral becomes

$$V = \frac{I\rho}{2\pi} \int_o^\infty \left[1 + 2\theta_1(\lambda)\right] j_o(\lambda r)\, d\lambda$$

(55)

this is the potential at the surface of the earth satisfying the specified condition.

Let $k(\lambda) = 1 + 2\theta_1(\lambda)$ (56)

so that the express for the potential becomes

$$V = \frac{I\rho}{2\pi} \int_o^\infty k(\lambda) j_o(\lambda r)\, d\lambda \quad (57)$$

K(λ) introduced into the resistivity theory by Slichter (in 1933) is called the Slichter Kernel function and $\theta_1(\lambda)$ is referred to as the Stefanescu Kernel function.

From the value of $\theta_1(\lambda)$, one can determine the value of K (λ) from the matrix.

The determinant of the matrix are the same except for the elements of the first column, such matrices can be added. The equation for the determinant and the relation of the elements in the matrices define the relation between Slichter function and the subsurface parameter ρ_1 and h_1

Resistivity Transform T (λ)

The Resistivity Transform T (λ) is defined in terms of Slichter Kernel function K (λ) as

$$T(\lambda)=\rho_1 K(\lambda) \tag{58}$$

The Apparent Resistivity Function

The Apparent Resistivity calculate from field observations by considering a symmetrical linear electrode arrangement with the current electrodes as shown below

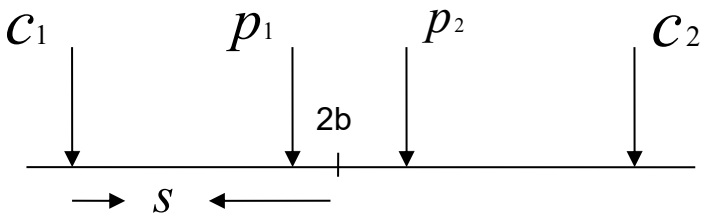

Figure 5. Symmetrical Schlumberger configuration

From the arrangement one can extra the following formula

$$\Delta V = \frac{I\rho}{2\pi}\left[\frac{1}{r_1}+\frac{1}{r_2}\right]-\left[\frac{1}{r_3}+\frac{1}{r_4}\right]$$
$$= 2\frac{I\rho}{2\pi}\left[\frac{1}{s-b}-\frac{1}{s+b}\right]$$

The expression for the apparent resistivity is then

$$\rho_a = 2\pi s\left(\frac{s^2-b^2}{4bs}\right)\frac{\Delta V}{I} \tag{59}$$

$Where\ \ 2\pi s\left(\frac{s^2-b^2}{4bs}\right)$ is the geometrical factor(k)

Relation between Apparent Resistivity and Transform Function for the Schlumberger electrode arrangement

The potential at the surface of a layered earth due to a point source of current is given by

$$V = \frac{I\rho}{2\pi}\int_o^\infty k(\lambda) j_o(\lambda r)\, d\lambda \tag{60}$$

using

$$V_{p_1} = V(s-b) - V(s+b)$$
$$V_{p_2} = V(s+b) - V(s-b)$$
$$\Delta V = V_{p_1} - V_{p_2}$$
$$\Delta V = 2\left[V(s-b) - V(s+b)\right]$$
$$\rho_a = 2s\left(\frac{s^2-b^2}{4bs}\right)\int_o^\infty k(\lambda)\left[j_o(\lambda s-\lambda b)\, j_o(\lambda s+\lambda b)\right] d\lambda$$

or
$$\rho_a = 2s\left(\frac{s2-b2}{4bs}\right)\int_o^\infty T(\lambda)\left[j_o(\lambda s-\lambda b) - j_o(\lambda s+\lambda b)\right] d\lambda \tag{61}$$

introducing the eccentricity $c = \frac{b}{s}$

$$\rho_a = 2s\left(\frac{\lambda - c^2}{4c}\right)\int_o^\infty T(\lambda)\left[j_o(\lambda s - \lambda b) - j_o(\lambda s + \lambda b)\right]d\lambda$$

For Schlumberger configuration

Assume that the distance between the potential /measuring electrodes is infinitesimal

$$k = \frac{s^2 - b^2}{4bs} \approx \frac{s}{4b}$$

Further, infinitesimal potential electrode spacing implies that, the electric field intensity in the region between the electrodes can be considered a constant. That is, the quotient

$$\frac{\Delta V}{2b} \to -2\left(\frac{\partial V}{\partial r}\right)_{r=s}$$

substituting these in equation (58)

$$\rho_{as} = \frac{2\pi s^s}{2I}\left[\left(-2\frac{\partial V}{\partial r}\right)_{r-s}\right]$$
$$= \frac{2\pi s^2}{r}\left(\frac{\partial V}{\partial r}\right)_{r=s}$$

Now substituting for v according to equation (59)

$$\rho_{as} = \frac{-2\pi s^2}{r}\frac{\partial}{\partial r}\left[\frac{I\rho 1}{2\pi}\int_o^\infty k(\lambda)\, j_o(\lambda r)d\lambda\right]_{r=s}$$

$$\rho_{as} = -s^2\rho^1\frac{\partial}{\partial r}\left[\int_o^\infty k(\lambda) j_o(\lambda r)d\lambda\right]_{r=s} \qquad (62)$$

There is a difficulty in differentiating the right numbers of this equation. One would be tempted to exchange /reveres the differentiation and integration process, that is, to differentiate under the integral sign.

The differentiation only affects the Bessel function J_0. From a theorem in Bessel function

$$\frac{\partial}{\partial \chi} j_o(\chi) = -j_1(\chi)$$

$$so\,that\;\; \rho_{as} = \rho_1 s^2 \int k(\lambda) j_1(\lambda s) \lambda d\lambda \qquad (63)$$

However, the infinite integral on the right hand side of equation (62) does not converge. For large values of λ, the amplitude of the Bessel function decreases as $\frac{1}{\sqrt{\lambda}}$ and consequently the product $\lambda j_1(\lambda s)$ steadily increases in amplitude. Since the Slichter Kernel function k(λ) is essentially finite, the integral thus diverges. (The mathematical background of this apparent discrepancy is that the right hand members of equation (61) do not satisfy the condition under which it is permissible to reveres the sequence of differentiation and integration).

The above difficulty is over come by using the Stefanescu Kernel Function $\theta(\lambda)$ rather than the Slichter Kernel function k (λ) it is known that as $\lambda \to \infty$ k (λ) $\to 1$ and $\theta(\lambda) \to 0$.

Hence, an infinite integral containing θ does converge. Thus, equation (58) becomes

$$\rho_{as} = -s^2 \rho_1 \frac{\partial}{\partial r} \int_o^\infty \left[1 + 2\theta_1(\lambda) j_o(\lambda r) d\lambda\right]_{r=s} =$$

$$-s^2 \rho_1 \frac{\partial}{\partial r} \int_o^\infty j_o(\lambda r) d\lambda - s^2 \rho_1 \frac{\partial}{\partial r} \left\{2 \int_o^\infty \theta_1(\lambda) j_o(\lambda r) d\lambda\right\}_{r=s}$$

using the Lipschitz Integral, that is,

$$\int_o^\infty e^{-\lambda z} j_o(\lambda_r)\, d\lambda = \frac{1}{\sqrt{r^2 + z^2}}$$

$$for\ z = 0$$

$$\int_o^\infty j_0(\lambda r)\, d\lambda = \frac{1}{r}$$

$$\rho_{as} = \left| -s^2 \rho_1 \frac{\partial}{\partial r}\left(\frac{1}{r}\right) - s^2 \rho_1 2 \frac{\partial}{\partial r} \int_o^\infty \theta_1(\lambda)\, j_o(\lambda r)\, d\lambda \right|_{r=s}$$

or after differentiating inside the integral sign

$$\rho_{as} = \rho_1 + 2s^2 p^1 \int_o^\infty \theta_1(\lambda s)\, j_o(\lambda_s)\, \lambda\, d\lambda$$

$$Since\ k_1 = 1 + 2\theta_1(\lambda)\ and\ T = \rho_1 k(\lambda)$$

$$\frac{T}{2\rho_1} - \frac{1}{2} = \theta_1(\lambda)$$

and $$\rho_{as} = \rho_1 + s^2 \left[T(\lambda) - \rho_1 \right] j_1(\lambda s)\, \lambda\, d\lambda \qquad (64)$$

This is the expression for apparent resistivity measured by the Schlumberger array at the surface of a horizontally stratified earth. The layer parameters ρ_i and h_i are contained in the resistivity transform T (λ). This is the expression used in direct interpretation of resistivity sounding field data using computers by the process of fitting the field curve to the one generated by the program through an iterative process.

CHAPTER THREE

DATA ACQUISITION, PROCESSING AND PRESENTATION

In the resistivity sounding survey the first step of collecting data was composed of instrument readings [voltage (V_p)] from the receiver and current (I) from the transmitter. Data processing was started by transforming the field data to the apparent resistivity (ρ_a) value using the relation

$$\rho_a = K \frac{v}{I}$$

3.1 Field Investigation and Instrument Used

The VES in this study was conducted using the symmetrical Schlumberger array. It is a popular method and has been extensively used as a standard tool for groundwater exploration. The Schlumberger soundings were carried with maximum current electrode spacing (AB/2) of 750m by injecting electrical current in to the ground by means of two outer electrodes, and the resulting potential difference or potential drop is measured by a second pair of potential electrodes placed near the center of the current electrodes. A series of measurements were taken by progressively increasing the current electrode separation and hence acquiring data from deeper and deeper horizons.

Generally, the field data acquisition was carried out by symmetrically expanding the array, between each measurement. Lines were selected such that for maximum line extension on both sides along the selected traverses, but it has been attempted to space the sounding points at 400m apart on the average.

In order to get an idea of the geological sequence subsurface and the associated resistivity values 18 vertical electrical sounding (VES) measurements were carried out along four lines and each of the lines were oriented across Mojo-Shenkora main road

that is directed in a NW-NE direction (see figure 2). The gravity survey was also carried out along those lines. Out of all gravity survey one was surveyed along the main road that runs NE-SW. Every VES station orientation of electrodes spread was made more or less in the same direction so as to minimize resistivity variations that may arise due to an isotropic nature of the subsurface formation.

The maximum number data points that can be memorized is 1566. These data stay in the in memory even after the machine is turned off or in case of a flat batter; a special procedure permits its subsequent cancellation. The instrument is completely controlled and programmed by a keyboard with four buttons integrated on the frontal panel. For a good functioning of the keyboard, the buttons should be pressed in a resolute and non-persistent way. Each time a button is pressed the instrument makes a sound.

3.2 Data Reduction

The apparent resistivity values are plotted on bi-logarithmic transparent paper. In processing of the collected data, the apparent resistivity values on the ordinates and the electrode separation (AB/2) on the abscissa. In most cases the sounding curve is segmented due to overlap measurement and can not be interpreted as it is. To have precise interpretations the segmented curves were shifted to the small MN curve points, so that the effect could be quantified and corrections could be made in order to obtain a single smooth curve that could be processed with the computer using “RESIST” software (Velpen, 1988).

3.3 Data processing and presentation

After data reduction was taken on each sounding curves, the data were processed using computer software called RESIST (Velpen, 1988) to determine the layer parameters, thickness and resistivities in the survey area.

Table 1. The GPS Location and elevation of the VES points

VES No	UTM coordinates (m)		Elevation (m)	Remarks
	Easting (E)	Northing (N)		
VES 1-1	518131	957237	2005	
VES 1-2	518549	957269	2005	
VES 1- 3	518942	957329	1988	
VES 1- 4	519469	957411	1983.5	
VES 1- 5	519945	957326	1996	
VES 2-1	521018	957944	2040	
VES 2-2	519557	958012	2001	
VES 2-3	518863	958147	2012	
VES 2-4	517979	958135	1974	
VES 3-1	520886	959284	2020	
VES 3-2	520501	959469	2009	
VES 3-3	520091	959646	2010	
VES 3-4	519776	959796	2013	
VES 4-1	521962	961684	2081	
VES 4-2	521669	961905	2085.7	
VES 4-3	511366	962128	2091.7	
VES 4-4	521032	962377	2080	
VES 4-5	520365	962403	2047	

The model parameters which were obtained by curve matching and auxiliary point methods were used to obtain good starting for inversion process of the Schlumberger resistivity sounding data by the computer software program. All sounding data have been interpreted using this program.

Principle of Equivalence and Suppression

Equivalence and suppression are two basic phenomena that cause ambiguity and a non-unique solution in resistivity interpretation. Equivalence refers to the condition in which different combination of layer resistivities and thickness may lead to apparent resistivity curves which are within the accuracy of observation are indistinguishable although not identical.

Suppression refers to the condition in which the effect of this intermediate layer (thickness very small compared to its depth) in an apparent resistivity curve of ascending and descending type is small that its detection from the curve maybe impossible.

For certain relations of the parameters of a three layer section, changes in resistivity and thickness of the intermediate layer do not produce any noticeable change in the form of the sounding curves. In such case, it is not possible to distinguish between two different intermediate layers and error may be involved in the interpretation of such sections.

1) For H-and A- type curves
    - it is found that the form of the curves remains practically the same, if, within certain limits the value of h_2 and ρ_2 are multiplied by the same factor, that is, H-and A-type curves are practically the same as long as $h_2/\ \rho_2$ $(=S_2)$ remain the same.
    - These sections may be called to be equivalent with respect to S.
2) Also for K- and Q - type sections, the form of the curves do not appreciably change if h_2 is increased or decreased by a certain factor

- Thus if $h_2 \rho_2$ (= T_2) remains constant and any change of h_2 and ρ_2 separately do not produce any noticeable change in the form of the curve - such sections may be called equivalent with respect to T.

CHAPTER FOUR

INTERPRETATION TECHNIQUES

4.1 General

Interpretation of geophysical survey data can be completely objective or highly subjective. It can range from a simple inspection of a map or other necessary figures to a highly sophisticated operation involving skilled personnel and elaborate supporting equipment. Some interpretations require little understanding of the geology, however the quality of most interpretation is improved if the interpreter has a good understanding the geology involved.

Geophysical interpretation of vertical electrical sounding data determine the thickness and the resistivity of different horizons from studying of the VES field curves, and the use of these results to obtain a useful geological picture of the area under investigation.

Direct and indirect approaches are the two methods by which resistivities and thickness of the layers are determined. The Direct method provides procedure for obtaining the layer parameters directly from the apparent resistivity sounding measurements (Slichter, 1933; Pekeris, 1940). More improvements have been made by using intermediate function (Koefoed, 1968; Ghosh, 1971).

The indirect method involves the determination of the layer parameters simply by comparing the measured sounding with standard curves, or a model curve that is calculated from given layer parameters. It includes the curve matching methods, automatic forward and iterative methods. Curve matching methods includes complete curve matching, partial curve matching and asymptotic methods. Complete curve matching can be done with the help of available theoretical master curves. The automatic iterative methods are more efficient and are widely used nowadays.

The VES curves collected in the field were initially interpreted by using two layer master curves and auxiliary point charts using a procedure known as the curve matching technique (Bhattacharya and Patra, 1968). In this preliminary manual interpretation, the number of layers, their thickness and resistivities were obtained, and these parameters help to develop a conceptual multiplayer earth model of the investigated area.

The layer parameters so obtained have been used as starting model that is the layer parameters were input into an interactive least squares inversion program, RESIST (Velpen, 1988). The inversion algorithm generates theoretical Schlumberger apparent resistivity curves, and then adjust the starting model in a number of iterations until a satisfactory best fit between the observed (field curves) and computer generated theoretical sounding curves are obtained. However, due to the well-known problems of equivalence and suppression, the best-fit model may not necessarily agree with the geology of the area under investigation. Thus in orders to arrive at an accurate and reasonable conclusion, the VES curves were interpreted using the knowledge of the local geology.

Finally, to have a clear view of the subsurface geology, a geoelectric cross-section of the study area was constructed by correlating the interpreted true resistivity and thickness of adjacent soundings.

4.2 Curve Matching and Auxiliary point Chart Techniques

Contrary to the method of horizontal profiling in which the apparent resistivity is studied directly and qualitative conclusions are drawn about the geological sub-surface conditions, the method of electrical sounding furnishes detailed information on the vertical succession of different conducting zones and their individual thickness and true resistivities. For this reason, the method is particularly valuable for investigations on horizontally or nearly horizontally stratified ground.

From all the resistivity values measured at a station the so-called resistivity curves are constructed for each observation, by using half the distance between the current electrodes as abscissa and the resistivity value as ordinate. The curve is plotted on transparent bi-logarithmic paper and consists of ascending and descending smooth braches. The interpretation curve with the ultimate aim to determine the thick nesses and the true resistivities of the individual layers in the ground is carried out by means of master curves. Numerous master curves have been constructed for many different combinations of homogeneous isotropic layer with different thickness and risistivities. These curves are like wise drawn on a double logarithmic scale. The origin (the “cross”) corresponds to ρ_a=1 and AB/2=1. For the sake of convenience the resistivity ρ_1 and the thickness h_1 of the superficial layer are taken as units for the corresponding parameters of the subsurface layers. Due to this construction principle any resistivity curve plotted in the same scale can be compared by superimposition even if the values ρ_1 and h_1 are different.

A simplified set of master curves for two-layer coordinates consisting of a superficial bed underlain by a bottom layer or infinite thickness. The curves give the apparent resistivity for only a few resistivity ratios ρ_2 / ρ_1 (i.e. resistivities of the bottom layer) between 0 and ∞ as a function of AB/2 a family out of the many sets of master curves required for three-layer conditions are represented by a few curves. They are constructed for the condition ρ_3/ρ_1 and infinite thickness of the third layer.

The procedure for the interpretation of measured curves of the two and three layer type is similar. The working sheet with the measured resistivity curve is placed on top of the set of master curves and is moved to such a position that the measured curve coincides with one of the given or interpolated master curves. When the coordinate systems of the two sheets are parallel, then the coordinates of the “cross” read off the axes of the working sheet correspond to the true resistivity ρ_1 and the thickness h_1 of the superficial layer. The two–layer curve is completely solved after the determination of ρ_2.

This parameter is equal to that ρ_a read on the working sheet that is asymptotically approached by the matching master curves. For three layer conditions ρ_2 and ρ_3 are given by ρ_{values} which are asymptotically approached by the matching master curves for the second branch and for the third branch respectively. The thickness of the second layer is obtained by multiplying h_1 with the number in the circle on the matching curve for the last branch.

The interpretation of resistivity curves of multi-layer type is usually carried out with the so-called auxiliary point method in which two and three layer master curves are used in combination with auxiliary diagrams. Briefly the principle of the method is as follows:

The first step is to determine the thickness and resistivity h_1 and ρ_1 of the superficial layer and the resistivity ρ_2 of the second layer. Next these two-layer are combine into a replacement layer which, together with the third stratum constitutes a two layer problem again. Consequently the thickness of the replacement layer and ρ_3 can be determined by means of two layer master curves. There after the three upper strata are combined into a replacement layer and the thickness of that and ρ_4 are determined and so on.

Thus the resistivities of the individual layers are obtained successively during the calculation process while the thick nesses are obtained by appropriate correction of the thickness of the replacement layers by the auxiliary diagrams. The interpretation can be carried out in a similar way by using three-layer master curves and auxiliary diagrams. The auxiliary point method has been applied to resolve the resistivity curve. The first cross at the left indicates h_1 and ρ_1. The second and the third crosses correspond to thickness and resistivity of the replacement layers for the upper two, respectively the upper three strata.

The final results, the true resistivity and thickness of the individual layers, are presented in the conventional way by a block diagram that resembles a resistivity log in a borehole.

4.3 Assymptotic Technique

For a two-layer earth, the apparent resistivity can be given from the image theory as

$$\rho_a = \rho_1 \left[1 + 2 \sum \frac{{k_{12}}^n \left[\frac{AB}{2h_1} \right]^3}{\left[\left(\frac{AB}{2h_1} \right)^2 + 2n^2 \right]^{\frac{3}{2}}} \right] \quad (1)$$

From the previous discussion we see that the apparent resistivity varies for the different electrode spreads. When the electrode spacing is very small, that is $\frac{AB}{2} = 0$, the above expression becomes

$$\rho_a = \rho_1$$

Which implies that the subsurface consists of a homogeneous ground with resistivity ρ_1 and $\frac{AB}{2} \to \infty$, the expression reduces to

$$\rho_a = \rho_1 \left(1 + 2 \sum_{n=1}^{n=\infty} k_{12}^n \right)$$

$$Here: \sum_{n=1}^{n=\infty} k_{12}^n = k_{12} + k_{12}^2 + k_{12}^3 + \ldots$$

$$\cong \frac{k_{12}}{1 - k_{12}}$$

From Hummel's Image theory (1932)

$$k_{12} = \frac{\rho_2 - \rho_1}{\rho_2 + \rho_1} \quad (2)$$

$$\rho_a = \rho_1 \left[1 + 2 \frac{k_{12}}{1 - k_{12}} \right]$$

Therefore,
$$= \rho_1 \left[1 + 2 \frac{\rho_2 - \left(\frac{\rho_1}{\rho_2} + \rho_1 \right)}{\left(\rho_2 - \frac{\rho_1}{\rho_2} + \rho_1 \right)} \right]$$

$$\rho_a = \rho_2$$

That is to say, a very large spacing the apparent resistivity is equal to the resistivity in the lower formation.

The master curves are prepared with dimensionless coordinates by setting k_{12} = 0 constant in the expression, the equation can be written in functional form as

$$\rho_a = \rho_1 F \left[\frac{AB}{2h_1} \right]$$

Then by taking the logarithm of both sides the equation becomes

$$\log \rho_a = F \left[\left(\log \frac{AB}{2} - \log h_1 \right) \right]$$

$$\log \left[\frac{\rho_a}{\rho_1} \right] = F \log \left[\frac{AB}{2h_1} \right]$$

The above expression shows that plotting AB/2 against ρ_a on log-log scale gives curves of exactly the same shape as long as ρ_2/ρ_3 is constant. Changes in ρ_1 cause a shift of the curve upward or downward parallel to the ordinate and changes in h_1 shift the curve to the left or the right parallel to the abscissa.

Thus the form of VES curves plotted on a bi-log scale is independent of ρ_1 and h_1 if ρ_2/ρ_1 is constant. This also found to be valid for a multi layer geoelectric section.
Two sets of theoretical two layer master curves are available for:

a) Ascending type ($\rho_2/\rho_1 > 1$)
b) Descending type ($\rho_2/\rho_1 < 1$)

Two layer standard curves prepared with a computer are available as an aid to interpretation. A typical set of two- layer curves published by Orellana and Mooney (1966)

A part from the possibility that three layer, four-layer or in general multi-layer master curves could be drown with a computer using their corresponding formulas, the available two-layer curves could be used to plot three layer or four-layer curves for certain special cases.

The whole set of three–layer sounding curves are divided into four groups, depending on the relative values of ρ_1, ρ_2, ρ_3.

a) Minimum type or H-type ($\rho_1 > \rho_2 < \rho_3$)
b) Double ascending type or A-type ($\rho_1 < \rho_2 < \rho_3$)
c) Maximum type or k-type ($\rho_1 < \rho_2 > \rho_3$)
d) Double descending or Q-type ($\rho_1 > \rho_2 > \rho_3$)

There can be only eight types of four – layer curves from a combination of the curves of the type H, A, K and Q. These are HA, HK, AA, AK, HH, KQ and QQ.

In other way, the correct solution can be derived from VES curves in very short time by using computer program. In this case two computations are involved; first the determination of the resistivity transform from the sample values of the apparent resistivity by the application of a suitable linear filter. This computation requires the availability of filter for converting the apparent resistivity into the resistivity transform. For resistivities measurements made in Schlumberger configuration. Such a filter has been published by Ghosh (1970).

Briefly, the method consists of:

a) Assuming initial Modeling

Nowadays this method is replaced by inversion methods since it is time consuming and tedious, particularly when several layers are treated. For the starting model, auxiliary point method with additional geological information may be used.

b) The Inverse Approach

At present the inverse approach is widely applied tool in the interpretation of VES measurement. The adjustments of layer parameters are made by a computer to get the best fit between measured and calculated curves, the number of layers during the iteration process will not be changed but the program has the option of assuming a fixed value for the layer parameters which is extremely useful when one or both of these parameters is already known.

The fitness between measured and calculated apparent resistivity values in evaluated by the standard deviation, that is, the lower root mean square of error (RMS error) the better the fit. The fit also depends on the initial guess of the layer model.

CHAPTER FIVE

RESULTS AND INTERPRETATION

In the following sections the geoelectricsections along the four traverses over which the sounding points were laid out are discussed separately. These sections were constructed after the data from each of the sounding points have been interpreted separately and the resistivities and thickness of the subsurface layers beneath the sounding points have been determined.

5.1 Line 1 (VES Points 1- 5)

Beneath line 1 the top dry soil (layer 1) cover is characterized by 3 to 36 Ωm resistivity, which is nearly 0.5 to 2m thick. Second to the topsoil, a layer whose thickness is ranging from 2 to 37m and resistivity between 19 to 65Ωm. beneath each VES point layers are covered by different types of rocks. Under VES points 1, 2- 3 and 4 - 5 the layer is may be covered by slightly fractured basalt, slightly fractured moist ignimbrite and fractured ignimbrite rocks respectively.

The third layer consists of different types of rocks. Beneath VES point 1 this layer has 22 Ωm resistivity and 4m thickness could be related to a wet fractured basalt rock. Laterally next to this layer a horizon with resistivity varying from 183 to 199 Ωm and thickness from 53 to 77m is may be identified as relatively resistive gnimbrite, but the third layer of

VES points 4 and 5 resistivity varies from 40 to 66 Ωm with uniform thickness of about 9m is probably characterized as slightly fractured ignimbrite rocks.

A fourth layer beneath VES point 1 has (72Ωm) with thickness 62m may be identified as slightly fractured ignimbrite. Just below VES points 2 and 3 this layer has uniform depth of 90m and the resistivity ranging from 48 to 62Ωm, may be identified as highly fractured ignimbrite rocks and the layer resemble a favorable water-bearing horizon. The fourth layer beneath VES points 4 and 5 has a thickness of 18 to 26m and resistivity 73 to 110 Ωm. The layer probably characterized as slightly fractured ignimbrite.

The fifth layer beneath VES point 1 has a resistivity of 57Ωm at depth of 75m. May be it represent highly fractured ignimbrite rocks and it could be refer water-bearing zones. The fifth layer of VES points 4 and 5 may be attribute highly fractured basalt with uniform resistivity of 16 Ωm at the depth of 26m and 31m respectively. The last layer of VES point 5 at the depth of 119m has a resistivity of 106Ωm. The layer is identified as relatively resistive ignimbrite.

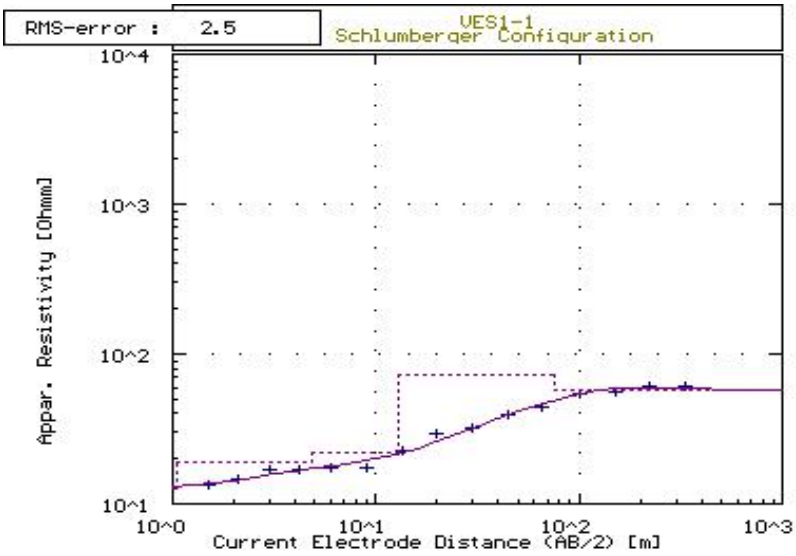

No	Res	Thick	Depth
1	12.6	1.0	1.0
2	18.7	3.8	4.8
3	22.0	8.0	12.9
4	72.3	62.0	74.8
5	56.9	-.-	-.-

Figure 6

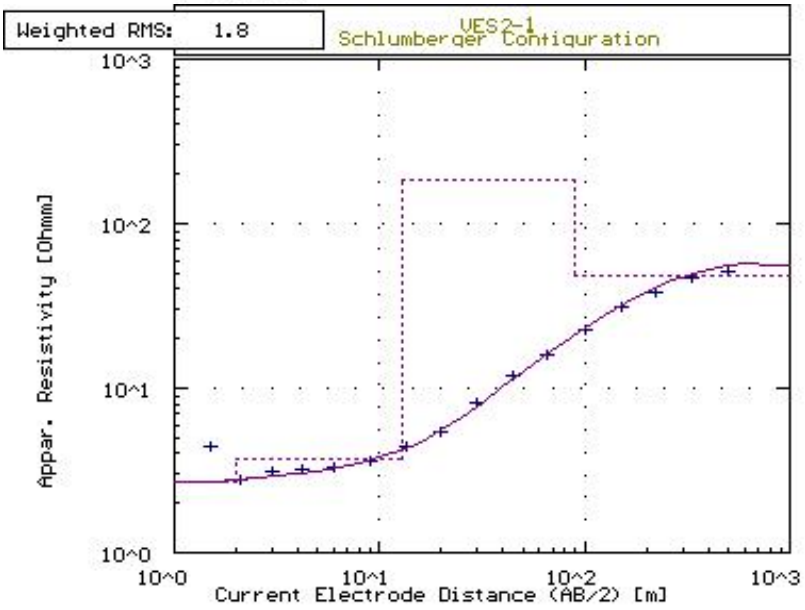

No	Res	Thick	Depth
1	2.7	2.0	2.0
2	3.7	10.9	12.9
3	183.2	76.6	89.5
4	48.0	-.-	-.-

Figure 7

Figures 6, Resistivity Sounding Curves along Line 1

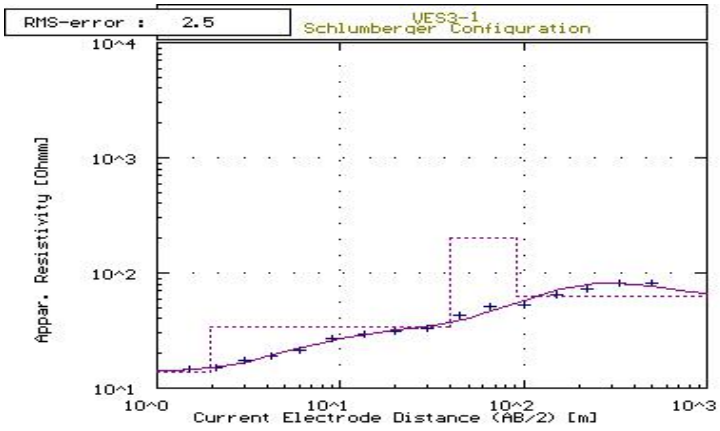

No	Res	Thick	Depth
1	13.8	1.9	1.9
2	34.2	37.3	39.2
3	189.3	52.7	91.9
4	62.4	-.-	-.-

Figure 8

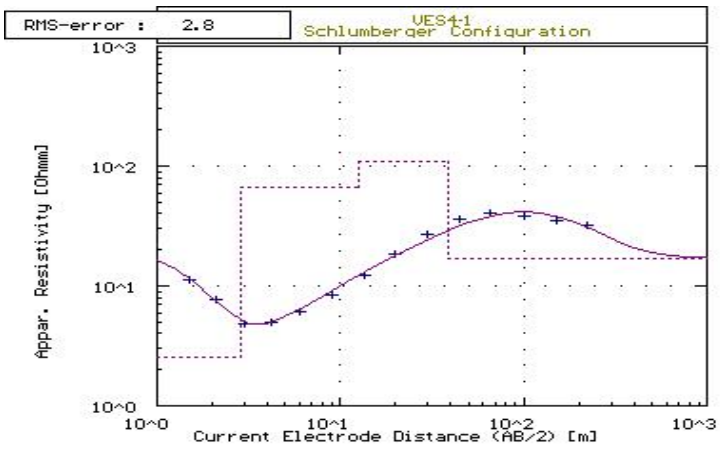

No	Res	Thick	Depth
1	21.9	0.7	0.7
2	2.5	2.1	2.8
3	66.3	9.8	12.7
4	109.8	25.7	38.3
5	16.8	-.-	-.-

Figure 9

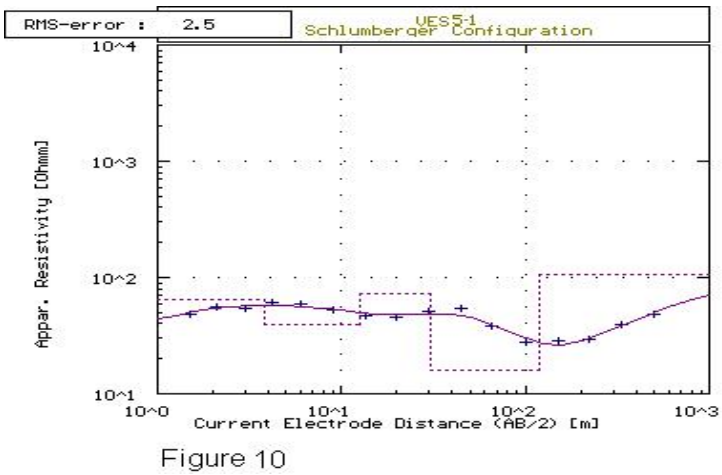

No	Res	Thick	Depth
1	35.8	0.5	0.5
2	65.0	3.3	3.8
3	39.6	8.8	12.6
4	72.9	18.2	30.8
5	15.8	88.6	119.4
6	105.6	-.-	-.-

Figure 10

Figures 8-10. Resistivity Sounding Curves along Line 1 (Contd.)

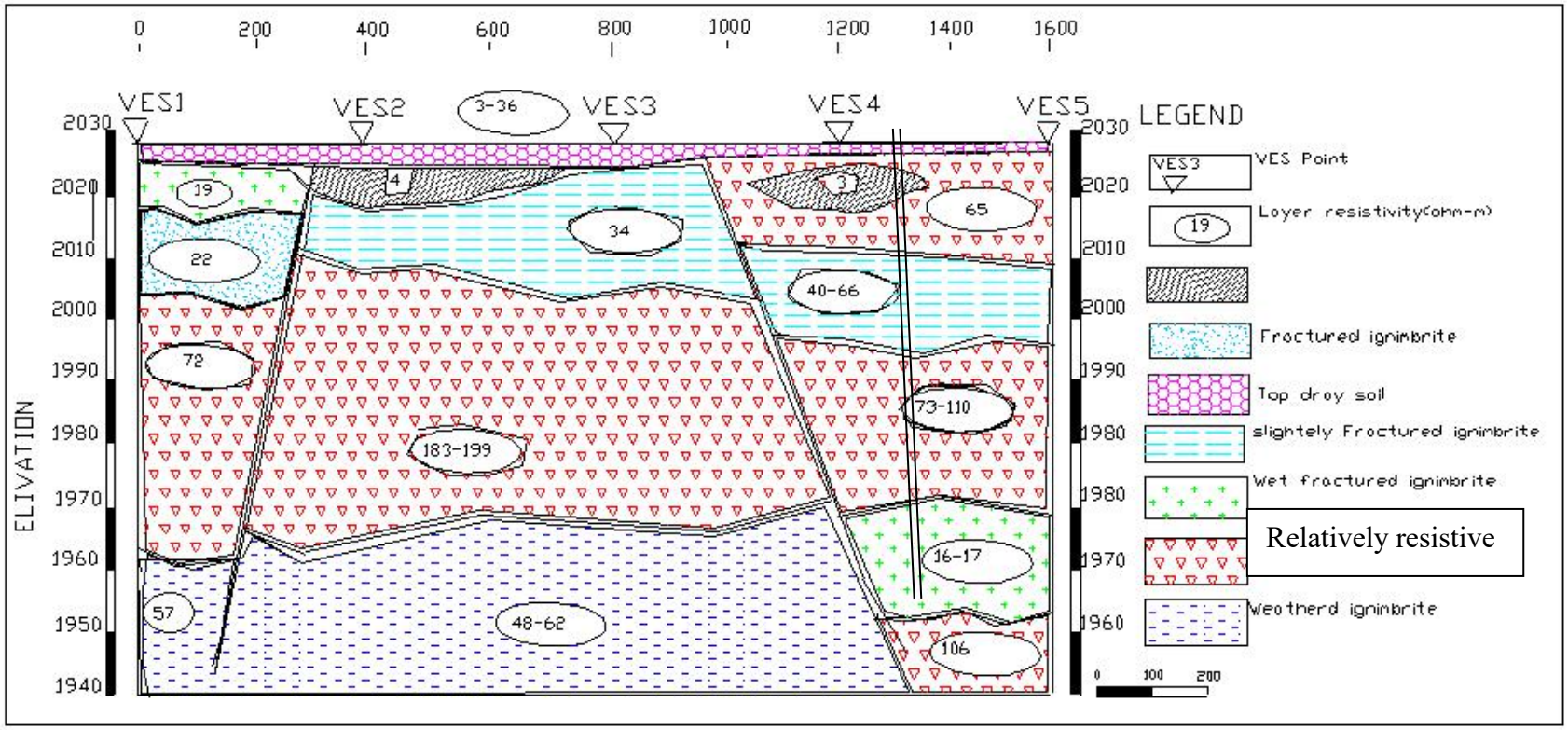

Figure 11. Geoelectric Section of Line 1

5.2 Line 2 (VES Points 1- 4)

The interpreted geoelectric section along Line 2 highlights five different resistivity layers. This section is given in Figures 16. The resistivity of the uppermost layer, ranges between 8 to 14 Ωm, and has an average thickness of 1m. It may be represents the top dry soil.

Beneath the top layer, layer of VES points 1, 2 and 3 may be characterized as low resistive basaltic rock rich in mo isture and that ranges from 2 to 4 Ωm and its thickness. The second layer under VES point 4 has a resistivity of 36 Ωm with thickness 32m is may be grouped as slightly fractured ignimbrite material. Here as shown on the geoelectricsection map there is a fault between VES points 3 and 4 starting from bottom of layer two and extend to the next layer.

The third layer beneath VES points 1, 2 and 3 resistivity ranges from 21 to 27 Ωm and has a thickness of varies from 25 -30 m. Depending on geology of the area it could be related to the response of weathered ignimbrite rock where as the third layer of around VES point 4 has a thickness of 14m with 11 Ωm resistivity probably identified as highly weathered basalt.

The thickness of the fourth layer varies from 104 to 125m and resistivity ranges between 110-120Ωm and it could be related to relatively resistive ignimbrite rocks.

The fifth or bottom substratum along the line lies at an average depth of 152m with resistivity varying from 27 to 47 Ωm and it may be attributed to a highly weathered ignimbrite which is uniformly distributed over the area. From the available subsurface geological information, it may be related to a highly saturated weathered ignimbrite zone. Also the uniform resistivity of this layer may indicate the resemblance in water bearing capacity.

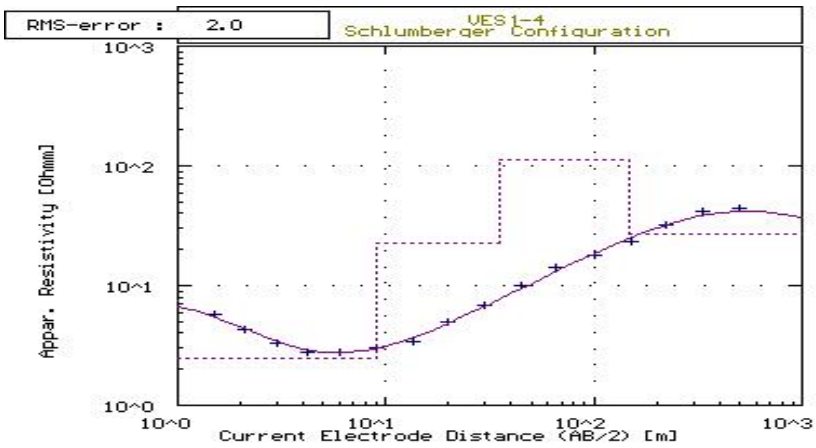

No	Res	Thick	Depth
1	7.5	0.9	0.9
2	2.4	8.2	9.1
3	22.6	25.8	34.9
4	112.5	114.0	148.9
5	26.6	-.-	-.-

Figure 12

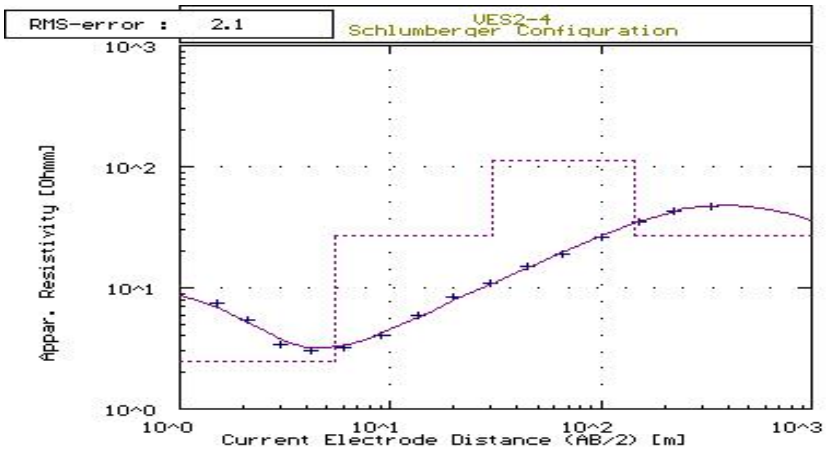

No	Res	Thick	Depth
1	10.2	0.8	0.8
2	2.5	4.7	5.5
3	26.6	25.2	30.6
4	111.5	112.2	142.8
5	26.7	-.-	-.-

Figure 13

Figures 12, 13. Resistivity Sounding Curves along Line 2.

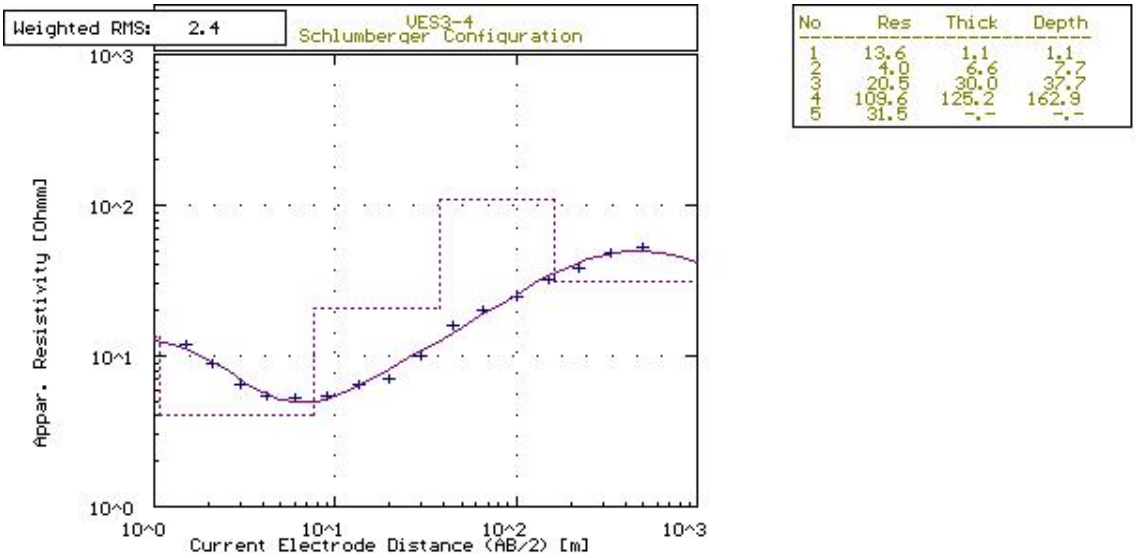

Figure 14

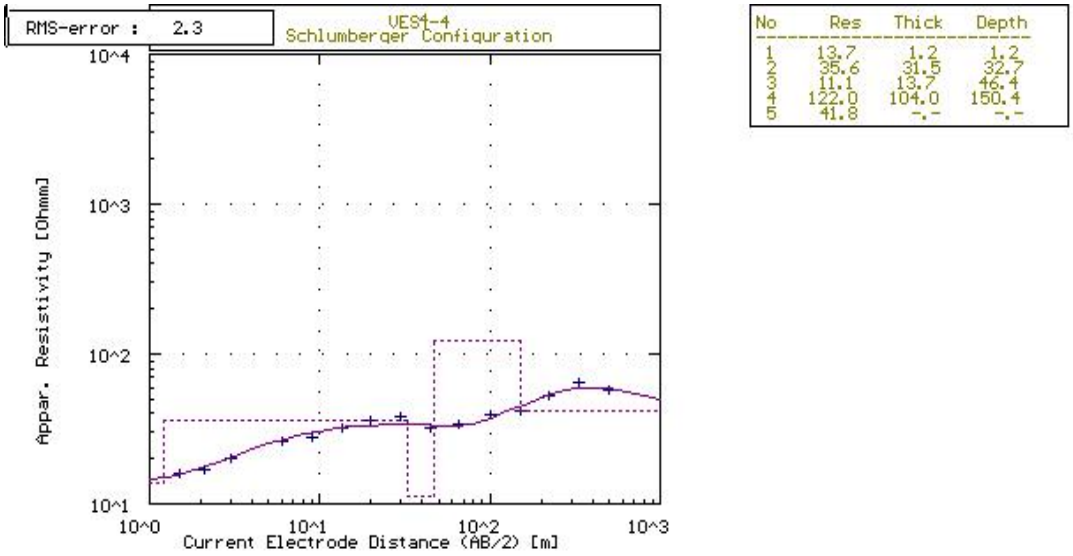

Figure 15

Figures 14, 15. Resistivity Sounding Curves along Line 2.

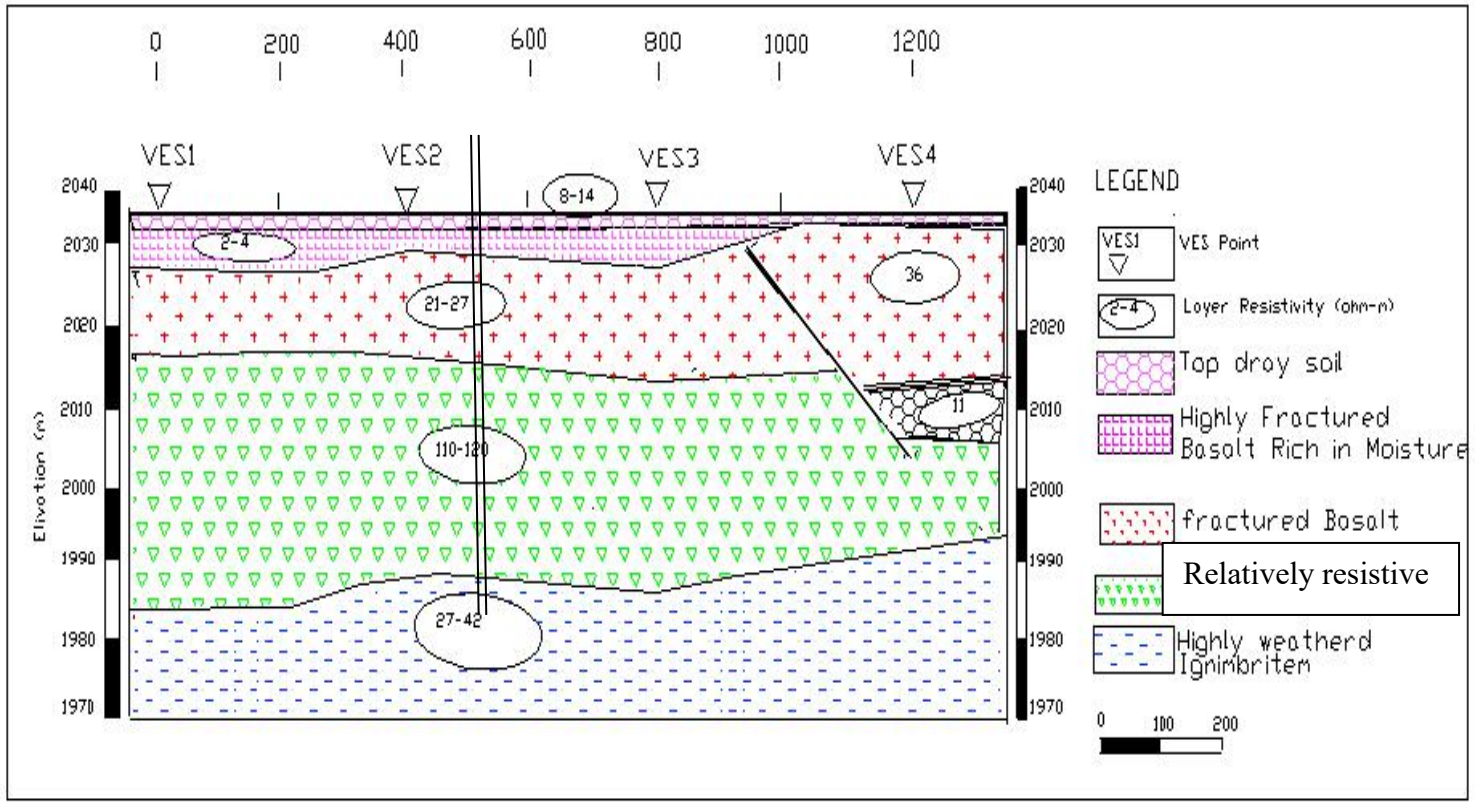

Figure 16. Geoelectric Section of Line 2.

5.3 Line 3 (VES Points 1-4)

The topmost part of the geoelectric section resistivityt ranges from 12-17Ωm. This layer is probably related to dry topsoil with average thickness of only about 1m. The second layer below VES points 1, 2 and 3 has very low resistivity that range between 3 to 5 Ωm with thickness varying from 3 to 5 m. This low resistivity informs that the layer could be grouped as highly weathered basalt rich in moisture. This layer beneath VES point 4 has a thickness of 41m with 51 ohm-m resistivity and it may be represent slightly fractured ignimbrite rock.

The third layer shows large lateral variations of resistivity ranging from 8 to 76 ohm-m over the area. Beneath VES points 1,2 and 3 this layer has a resistivity ranging from 32 to 76 ohm-m with thickness varying from 14-20m and it could related to slightly fractured ignimbrite. Beneath VES point 4 the layer has aresistivity of 8 ohm-m with thickness 19m resembles as highly weathered basalt rich in moisture. As the geoelectricsection map (Figure 21) shows, there are two faults starting from the bottom of layer one and extending down.

The fourth layer has beneath VES point 1 and 3 the resistivity ranging from 158 to 197 ohm-m and a thickness varying from 82-167m. This layer may be identified as relatively high resistivity ignimbrite. The forth layer of ves point 4 has resistivity 75 ohm-m and thickness 82m could be related to slightly fractured ignimbrite. Beneath VES 2 this layer has a resistivity of 197Ωm and thickness 166m may be identified as fractured ignimbrite rocks.

The fifth or bottom substratum layer is marked by moderate resistivities that range from 28 to 43 Ω m with average depth of 160 m. This layer could be related to highly weathered ignimbrite and likely water-bearing horizon along the traverse.

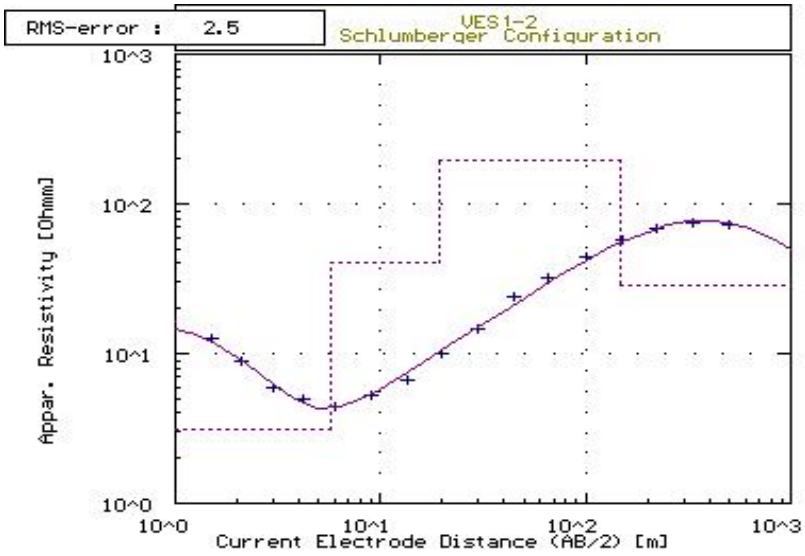

No	Res	Thick	Depth
1	16.5	1.0	1.0
2	3.1	4.8	5.8
3	40.1	13.5	19.3
4	197.1	128.9	148.2
5	28.2	-.-	-.-

Figure 17

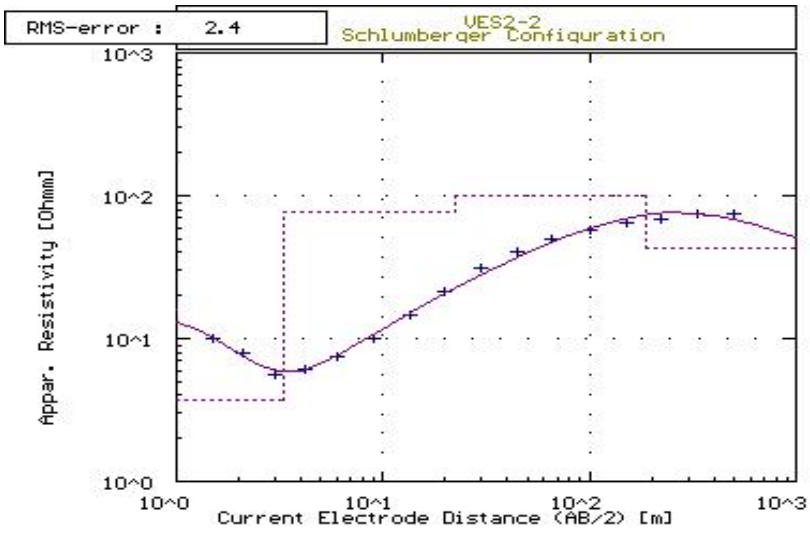

No	Res	Thick	Depth
1	15.9	0.8	0.8
2	3.7	2.5	3.3
3	75.9	19.0	22.3
4	99.9	166.5	188.7
5	42.8	-.-	-.-

Figure 18

Figures 17, 18. Resistivity Sounding Curves along Line 3.

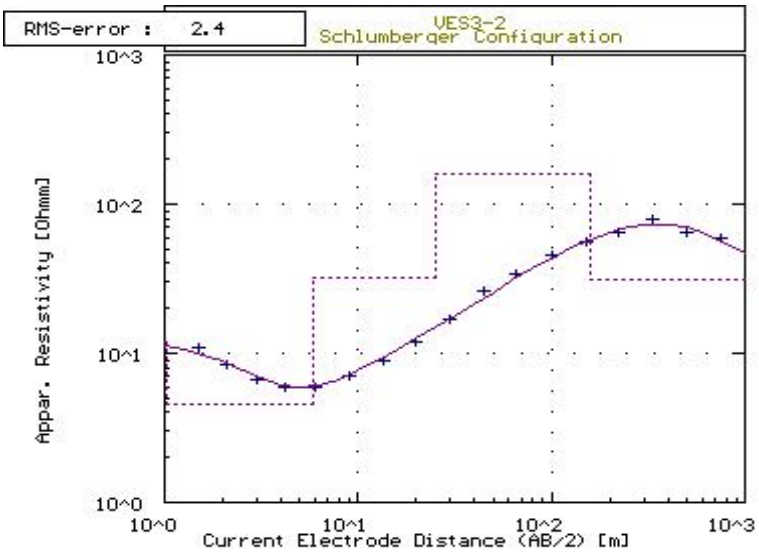

No	Res	Thick	Depth
1	12.1	1.0	1.0
2	4.6	4.8	5.8
3	31.9	19.4	25.2
4	157.6	134.9	160.1
5	30.9	-.-	-.-

Figure 19

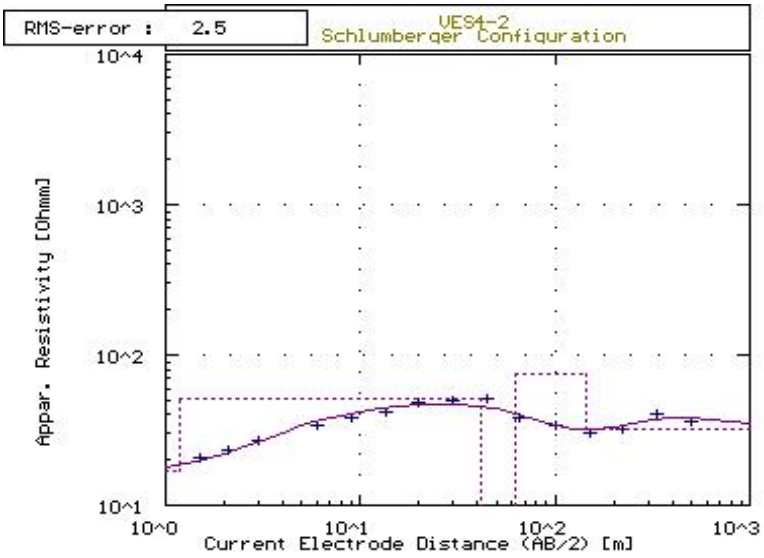

No	Res	Thick	Depth
1	16.9	1.2	1.2
2	50.7	40.7	41.9
3	7.6	19.9	61.7
4	75.2	82.3	144.0
5	31.9	-.-	-.-

Figure 20

Figures 19, 20. Resistivity Sounding Curves along Line 3.

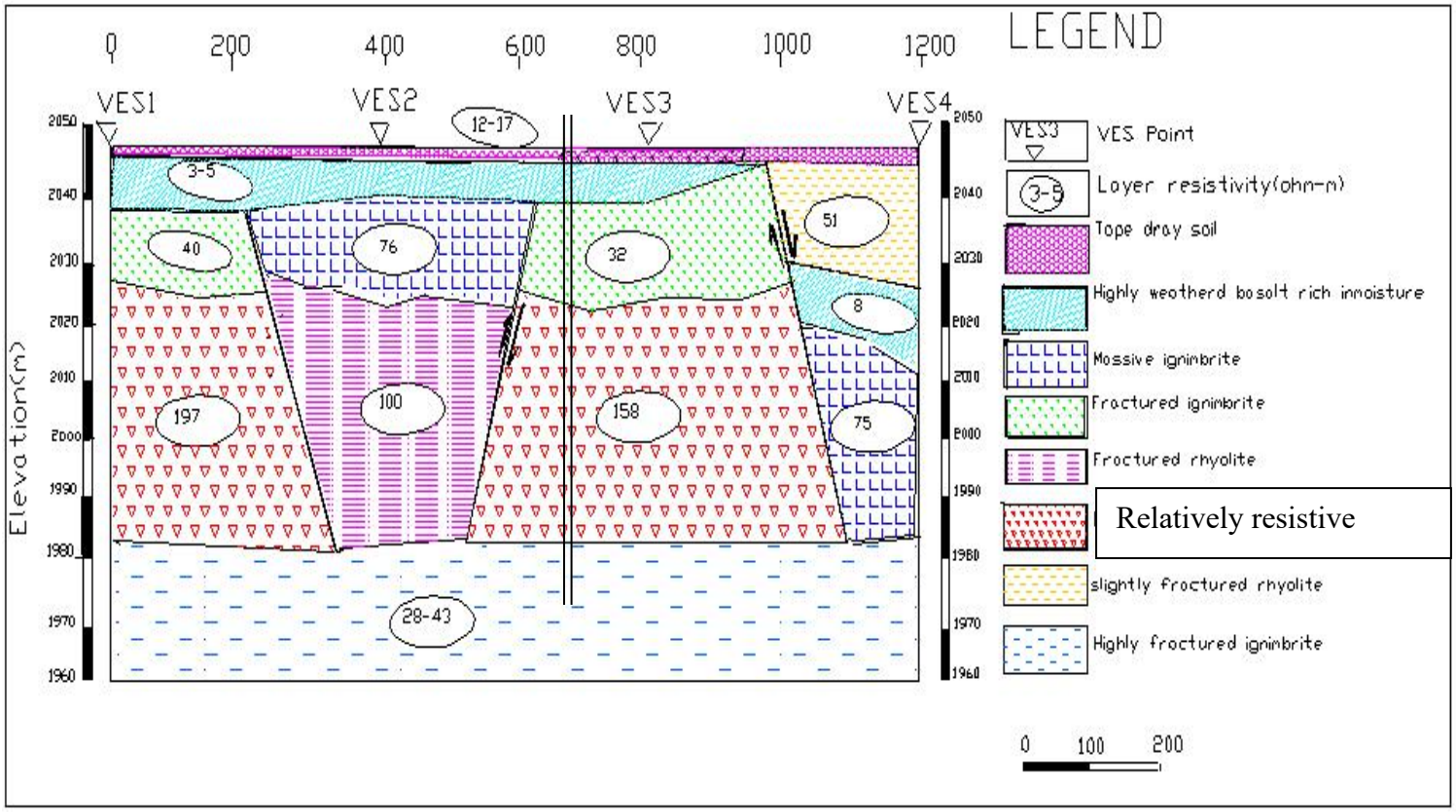

Figure 21 Geoelectric Section of Line 3.

5.4 Line 4 (VES Points 1-5)

Along this line there are 5 VES points, the geoelctricsection is constructed from data of Figures 22-26 and the section is given as Figure 27. The top layer along this line is characterized by resistivities ranging between 10 to 51 Ωm and soil whose thickness varies between 0.6 to 2.7m. This topsoil is underlined by lower resistivity layer of 4 to 15Ωm and thickness ranging between 1 to 11m which is probably composed of highly fractured basalt.

The third layer shows large lateral variations in resistivity and describes a transition from relatively resistive ignimbrite (98 ohm-m) beneath VES point 1 to less resistive weathered basalt zone (ranging from 20 to 31Ωm) beneath VES points 2, 3, 4 and 5. the layer has nearly uniform thickness and is about 24 to 34m throughout this layer, but this laterally high ranging resistive layer is divided by a fault starting from the end of layer one between VES points one and two and extends down to other layers as shown in figure 27, due to the formation of this fault the layers below VES point 2, 3, 4 and 5 may slide down.

The fourth layer also shows large lateral variations in resistivity and transforms from less resistive weathered basalt rock (38 Ω m) to relatively resistive (ranging from 93 to 161 Ω m) ignimbrite layer beneath VES points 2, 3, 4 and 5. It is nearly uniform in thickness and is about 95 to 126m beneath VES points 1, 3, 4 and 5 but below VES point 2 is 174m.

The bottom layer, whose resistivity values range between 20 to 33 Ω m and depth extending from 126 to 216m beneath VES point 2, 3, 4 and 5 may be related to a highly weathered ignimbrite water-bearing formation. Below VES point 5 the layer may be slightly weathered rhyolite ignimbrite (58Ωm) at the depth point of 139m.

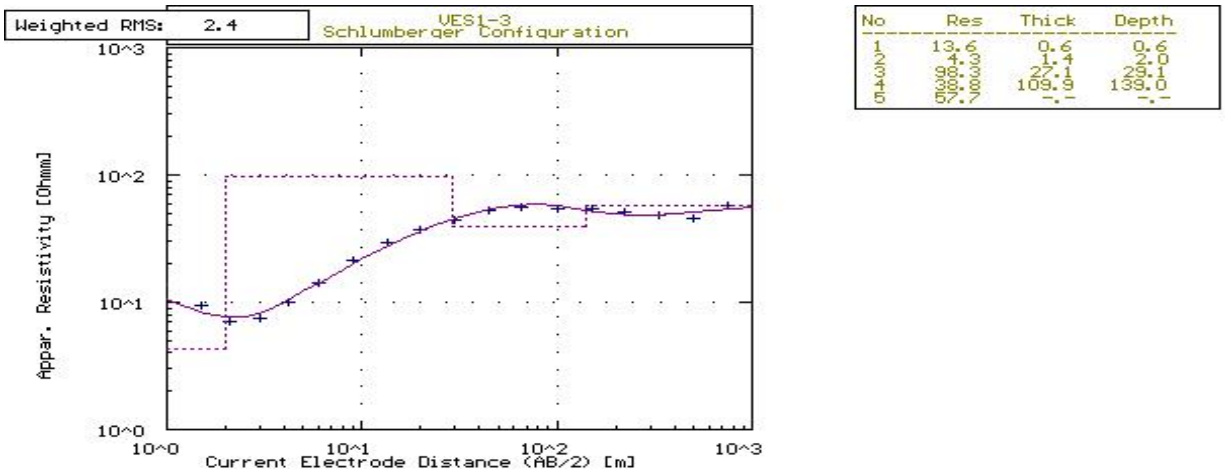

Figure 22

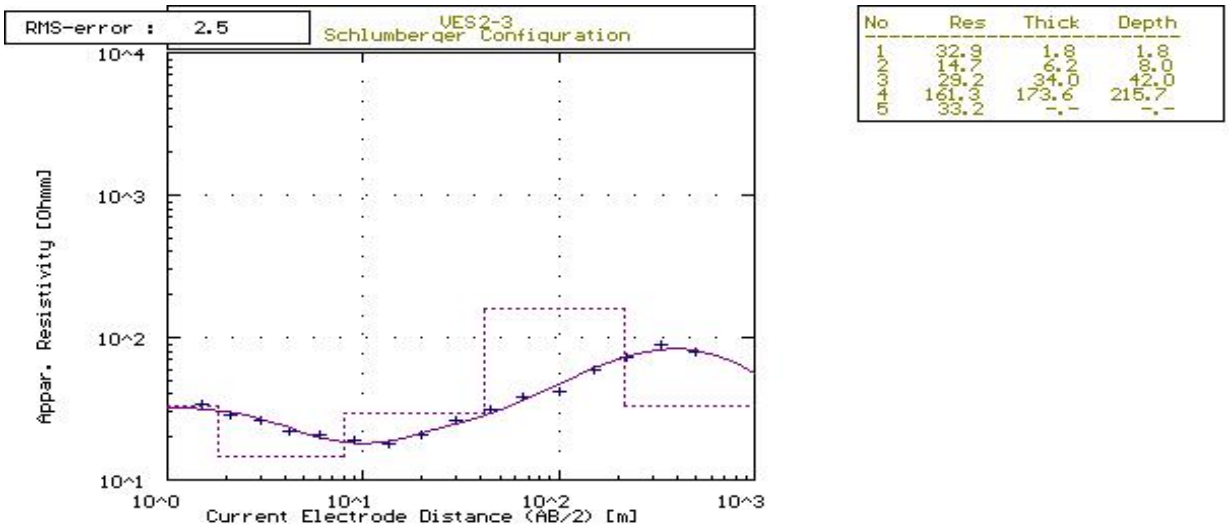

Figure 23

Figures 22, 23. Resistivity Sounding Curves along Line 4.

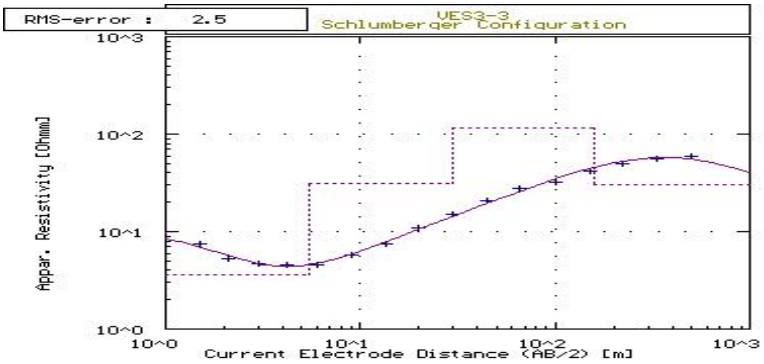

No	Res	Thick	Depth
1	9.6	0.8	0.8
2	3.0	4.5	5.4
3	31.4	24.4	29.9
4	115.4	126.8	156.7
5	30.2	-.-	-.-

Figure 24

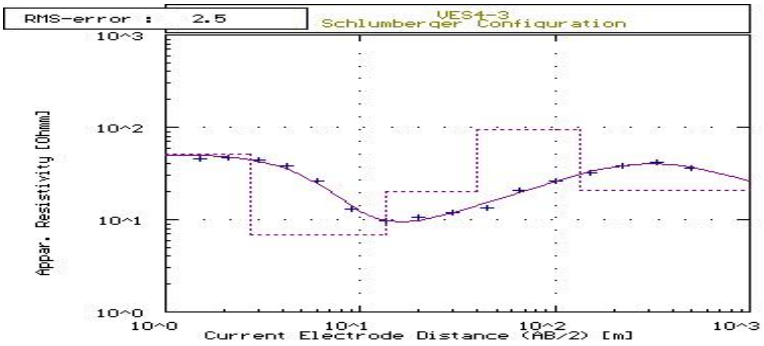

No	Res	Thick	Depth
1	50.8	2.7	2.7
2	6.0	10.8	13.5
3	20.0	26.1	39.6
4	99.2	95.1	134.7
5	20.8	-.-	-.-

Figure 25

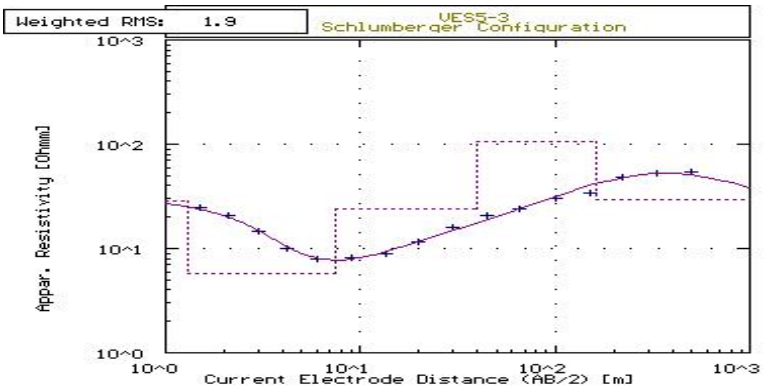

No	Res	Thick	Depth
1	28.3	1.3	1.3
2	5.0	5.1	7.4
3	23.0	32.2	39.6
4	104.6	123.2	162.7
5	29.7	-.-	-.-

Figure 26

Figures 24-26. Resistivity Sounding Curves along Line 4 (contd.).

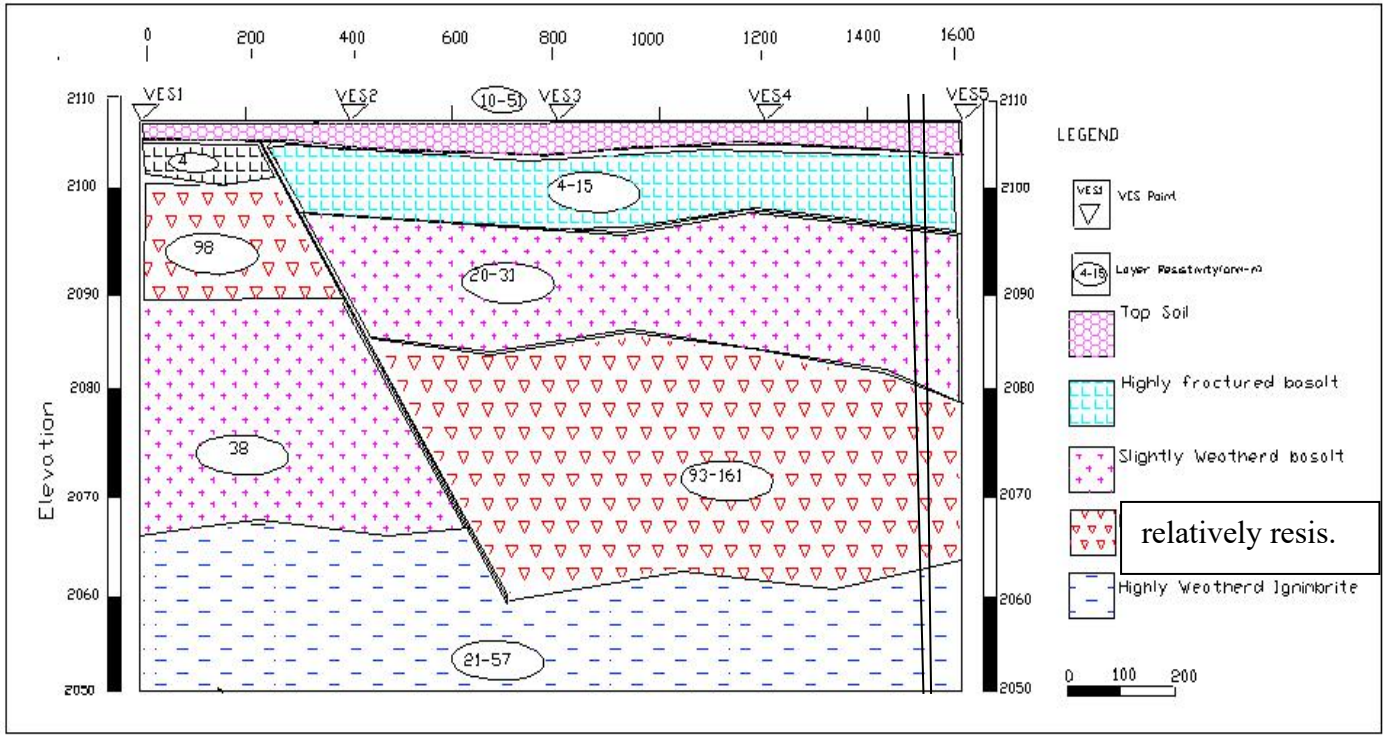

Figure 27. Geoelectric Section of Line 4

CHAPTER SIX

CONCLUSIONS AND RECOMMENDATIONS

The geological sounding curves can yield the information that consists of the data about the number of layers, their thickness, and resistivity values when it is incorporated with external geological information. The information about the top layer, the bottom layer, and the possible strata in between can be derived from the VES curve itself with out any external information.

During the interpretation phase, maximum effort was put into correlating the electric resistivity survey result to the hydrogeology of the area. Based on the interpretation, the following conclusions have been drawn using the integrated approach:

1. As shown from the results of the electrical resistivity surveys, the area is highly affected by fracturing and faulting. Detected faults and fractures control the flow of groundwater. Most of the ignimbrite rocks are highly fractured and are expected to be the water-bearing horizons at different depths below each VES point.
2. From geological, hydrogeological and resistivity works, almost in every part of the study area, there are topsoil, basalt, ignimbrite and rhyolitic ignimbrite rocks. Geologically the ignimbrite rocks are older than the over lying basalt rock.

3. The geological structures (fractures, faults, and contacts) play a great role in the movement and occurrence of the groundwater in the study area. The ignimbrite and its horizontal bedding contribute more for the recharge and movement of the groundwater through the faults and weak zones, whereas the contacts also generated due to these faulting act as barriers as well as conduits for the groundwater flow.

4. Around 10 km far from the study area, a new drilled borehole has a discharge of 6.6 L/sec. Therefore, with proper location of the boreholes to be drilled there is a strong possibility to supply this severely affected area with adequate water supply from the subsurface.

5. In such structurally controlled area characterized by arid zone climate, it is almost impossible to detect the groundwater table only through surface geological surveys and the use exploration geophysics becomes essential.

6. The depths to water bearing horizons over the survey traverses are as follows

- Line one: at the marked position to a depth of between 75 to 91 m (Figure 11)
- Line two: to a depth ranging between 144 to 163 m (see Figure 16)
- Line three: a borehole preferably sunk to a depth of ranging between 144 to 189m may give water (Figure 21), and
- Line four: water-bearing horizon is encountered at much deeper zone in this area and groundwater may be extracted at minimum depth of 127m and this may extend to the maximum depth of 216 m in some locations along the line (Figure 27).

Recommendations:

Based on the outcomes of this study, the following recommendations are forwarded.

1. The fractures and weak zones are the major controls for the flow of groundwater over the area. The main geologic units encountered over the survey area are basalt, ignimbrite and rhyolitic ignimbrite rocks covered and the potential water bearing horizon is the fractured ignimbrites.

2. On the basis of the study, if a need arises for drilling productive groundwater wells, it would better be along the geophysical detected faults and weak zones

and preferably at the borehole sites marked on the respective geoelectric sections.

3. The regional water development bureau is to be encouraged to sink a test well on one of the potential borehole sites located by our survey to validate the results.
4. The interpretations of the gravity surveys will confirm the presence of the faults interpreted from the geoelectical surveys and further improve the conclusions of this work, i.e. that structures control the ground water regime over the Shenkora area.

5. In order to map the networks of fractures and faults in much detail additional geophysical methods must be employed, like for example resistivity profiling surveys and magnetic surveys. .

REFERENCES

A.A.R. Zohdy. G.P. Eaton and D.R. Mabedy., Application of surface Geophysics to Ground-water investigations. United State Department of the interior Rogers C.B. Morton, secretary.

Alem Tiruneh ,(2004). Hydrogeology of Modjo River Catchment, M. Sc.Thisis.

Carpenter, E.W. and Habber Jam, G.M., (1956a), Tri-potential method of resistivity prospecting Geophysics.

Dobrin, M.B, (1976), Introduction to Geophysical prospecting, 3rd edition, Mc Graw-Hill, New York.

Eduards L.S., (1977), A modified pseudo section for resistivity and induced- polarization. Geophysics', 42, 1020-1036.

Emilia, D.A., Last, B.J and authored, A.K. (1976), Geophysical exploration for groundwater in Ethiopia. Bull. Geophysics.

Getachew H/Michal, (2004), Study on Groundwater and requirements for drilling and other systems tapping groundwater in Ethiopia.

Hummel; J.N., (1932), A theoretical study of apparent resistivity in surface potential methods. V.27, p.667-690.

John M. Reynolds. (…), An Introduction to Applied and Environmental Geophysics. Reynolds Geo-sciences Ltd. UK

Kazmin, V., (1975), Exploration of the Geological map of Ethiopia. Ethiopian Institute of Geological Surveys. Bulletin No. 1, 00.1-14.

Kazmin, V., (1979), Explatory notes of the geological map of Ethiopia, ministry of Mines and Energy.

Keary, P. and Brooks, M., (1984), An Introduction to Geophysical Exploration. Black well Scientific publications, Oxford London Edinburgh

Koefoed, O., (1979), Geosounding PrinciplesI, Resistivity sounding measurements. Elsevier, Amesterclam.

Koefoed, O., 1968. The applications of the Kernel function in interpreting geoelectrical resistivity measurements. Geberder Borentraeger, Berlinstuttgart.

Kramvis, S.C., 1987. Application of Electrical Resistivity in Groundwater Exploration in Cyprus. Ph.D. Thesis, Leicester Univ.

Mohr p.a.,(1971). Ethiopian rift in and plteaus: Some volcanic petrohemical defferences.J. geophys.Res., 76,1967-1884.

Moony, H.M. and Wetzel, W.W, 1956. The potential about a point electrode and apparent resistivity curves for a two, three and four layered warth. The University of Minnesota Press, Minneapolies.

Mundry, E., 1980-short note on the effect of finite distance potential electrodes on Schlumberger resistivity, measurements- a simple correction gloph . Geophysics, V.45, PP.1872-1875.

Parasnis, D.S.1962, Principles of applied geophysics (3rd edition) champ man and Hall, London, PP. 98-212.

P.K. Bhattacharya and H.P. Patra. (1968), Direct current Go electric sounding principles and Interpretation. Department of Geology and geophysics, Indian Institute of Technology, Kharagpur, west Bengal, India.

Slichter, L.B., 1933. The interpretation of the resistivity prospecting method for horizontal structures. Physics, V.4, P.307-322.

Telford, W.M.; Geldart, L.P. and Sheriff, R.E. 1976. Applied Geophysics. (4th edition). Cambridge University press, Cambridge, pp 677-686.

Declaration

This thesis is my original work and has not been presented for a degree in any other university, and that all sources of material used for the thesis have been duly acknowledged.

Dr. Tigsitu Haile (Adviser)

Signature_____

Minilik Wube

Signature_____

Data and place of submission, July 2005, Addis Ababa.